Meron-Cluster Approach to Systems of Strongly Correlated Electrons

S. Chandrasekharan[a], J. Cox[b], J.C. Osborn[a*] and U.-J. Wiese[b,c]

[a] Department of Physics, Box 90305, Duke University, Durham, North Carolina 27708
[b] Center for Theoretical Physics, Laboratory for Nuclear Science and Department of Physics, Massachusetts Institute of Technology, Cambridge, Massachusetts 02139
[c] Institute for Theoretical Physics, Bern University, CH-3012, Switzerland

February 1, 2008

Abstract

Numerical simulations of strongly correlated electron systems suffer from the notorious fermion sign problem which has prevented progress in understanding if systems like the Hubbard model display high-temperature superconductivity. Here we show how the fermion sign problem can be solved completely with meron-cluster methods in a large class of models of strongly correlated electron systems, some of which are in the extended Hubbard model family and show s-wave superconductivity. In these models we also find that on-site repulsion can even coexist with a weak chemical potential without introducing sign problems. We argue that since these models can be simulated efficiently using cluster algorithms they are ideal for studying many of the interesting phenomena in strongly correlated electron systems.

*Current address Universiry of Utah, Salt Lake City, USA

1 Introduction

Strongly correlated electrons are among the most interesting condensed matter systems. In particular, the doping of anti-ferromagnetic cuprate layers leads to high-temperature superconductivity. Understanding the dynamics of strongly correlated electron systems is very challenging because perturbative analytic techniques fail for systems of many strongly coupled degrees of freedom. On the other hand, numerical simulation methods are applicable in these cases. Unfortunately, numerical simulations of models involving fermions are far from trivial. A standard technique is to linearize four-fermion interactions by the introduction of bosonic fields [1]. Then the fermions are integrated out, leaving behind a fermion determinant which acts as a non-local effective action for the bosonic fields. In some cases, for example, in undoped cuprate layers at half-filling, the fermion determinant is positive and can be interpreted as a probability for the bosonic field configurations. Then standard importance sampling techniques can be applied to the bosonic theory. Still, due to the non-locality of the effective action, such simulations are very time consuming. In other cases of physical interest — in particular for doped cuprates away from half-filling — the fermion determinant may become negative and can hence not be interpreted as a probability for the bosonic configurations. When the sign of the fermion determinant is included in measured observables, the fluctuations in the sign give rise to dramatic cancellations. As a consequence, the relative statistical errors of observables grow exponentially with the volume and the inverse temperature of the system. This makes it impossible in practice to simulate large systems in the low-temperature limit. In particular, the fermion sign problem prevents numerical simulations of the Hubbard model away from half-filling and is the major stumbling block against understanding high-temperature superconductivity with numerical methods.

Dealing with the fermion sign problem after the fermions have been integrated out is incredibly complicated since the resulting bosonic effective action is non-local. Before integrating them out, fermions are usually described by anti-commuting Grassmann variables which are practically impossible to simulate directly. Here we propose a different strategy. Instead of working with Grassmann coherent states, we formulate the fermionic path integral in the Fock state basis of the Hilbert space. Then a fermion configuration is described in terms of bosonic occupation numbers which define fermion world-lines. In this case, the bosonic occupation numbers interact locally. However, besides the positive bosonic Boltzmann weight, there is a fermion permutation sign that results from the Pauli principle. Two fermions that interchange their positions during the Euclidean time-evolution give rise to a minus-sign. In general, the fermion world-lines which are periodic in Euclidean time define a permutation of fermion positions. The sign of this permutation is the fermion sign. The resulting sign problem is often more severe than the one associated with the fermion determinant. For example, in the world-line formulation a sign problem arises for the Hubbard model even at half-filling, while the fermion determinant is

positive in that case.

Fortunately, in the Fock state basis the sign problem can be completely eliminated, at least in a large (but still restricted) class of models. This was first demonstrated for a system of spinless lattice fermions in [2, 3] by re-writing the partition function in terms of the statistical mechanics of closed loops with non-negative Boltzmann weights. Loops with a certain topology, referred to as *merons*, do not contribute to the partition function. A local algorithm was constructed in the loop space which avoided meron-clusters and thus solved the sign problem. It is well known that spinless fermions can be converted to relativistic staggered fermions by introducing carefully chosen phase factors with every fermion hop [4]. Using this strategy, the solution to the fermion sign problem with spinless fermions has been exploited to extensively study the critical behavior of a second order chiral phase transition in the universality class of the Ising model [5, 6, 7].

Here we extend these successful techniques to fermions with spin and, in particular, to systems in the Hubbard model family. Using a specific example, we show how one can build models so that the sign problem is completely solved. For technical reasons related to the details of the cancellation of signs, the method does not apply to the standard Hubbard model Hamiltonian. Additional terms must be included. Still, the modifications do not affect the symmetries of the problem and we believe that the physics of some of the models discussed here is qualitatively similar to the standard Hubbard model. It should be pointed out that there is no reason to concentrate on the standard Hubbard model except for the simple form of its Hamiltonian. The fact that for similar Hamiltonians our method can completely eliminate the sign problem and yield a very efficient fermion algorithm — which is not the case for the standard Hubbard model — is reason enough to replace the standard Hubbard model by a modified Hamiltonian. After all, we want to focus on understanding the general physical phenomena underlying high-temperature superconductivity — not necessarily on the details of one particular model Hamiltonian. Interestingly, in the modified model the sign problem can be eliminated even in the presence of an on-site repulsion at a finite chemical potential as long as a certain inequality is satisfied.

1.1 The Fermion Sign Problem

Let us first discuss the nature of the fermion sign problem. We consider a fermionic path integral

$$Z_f = \sum_{[n]} \mathrm{Sign}[n] \exp(-S[n]) \tag{1.1}$$

over configurations of occupation numbers n with a Boltzmann weight whose magnitude is $\exp(-S[n])$ and sign is $\mathrm{Sign}[n] = \pm 1$. Here $S[n]$ is the action of a corre-

sponding bosonic model with partition function

$$Z_b = \sum_{[n]} \exp(-S[n]). \tag{1.2}$$

A fermionic observable $O[n]$ is obtained in a simulation of the bosonic ensemble as

$$\langle O \rangle_f = \frac{1}{Z_f} \sum_{[n]} O[n] \mathrm{Sign}[n] \exp(-S[n]) = \frac{\langle O \ \mathrm{Sign} \rangle}{\langle \mathrm{Sign} \rangle}. \tag{1.3}$$

The average sign in the simulated bosonic ensemble is given by

$$\langle \mathrm{Sign} \rangle = \frac{1}{Z_b} \sum_{[n]} \mathrm{Sign}[n] \exp(-S[n]) = \frac{Z_f}{Z_b} = \exp(-\beta V \Delta f). \tag{1.4}$$

The expectation value of the sign is exponentially small in both the volume V and the inverse temperature β because the difference between the free energy densities $\Delta f = f_f - f_b$ of the fermionic and bosonic systems is always positive. Hence, the fermionic expectation value $\langle O \rangle_f$ — although of order one — is measured as the ratio of two exponentially small signals which are very hard to extract from the statistical noise. This is the origin of the sign problem. We can estimate the statistical error of the average sign in an ideal simulation of the bosonic ensemble which generates N completely uncorrelated configurations as

$$\frac{\sigma_{\mathrm{Sign}}}{\langle \mathrm{Sign} \rangle} = \frac{\sqrt{\langle \mathrm{Sign}^2 \rangle - \langle \mathrm{Sign} \rangle^2}}{\sqrt{N} \langle \mathrm{Sign} \rangle} = \frac{\exp(\beta V \Delta f)}{\sqrt{N}}. \tag{1.5}$$

The last equality results from taking the large βV limit and using $\mathrm{Sign}^2 = 1$. In order to determine the average sign with sufficient accuracy one needs on the order of $N = \exp(2\beta V \Delta f)$ measurements. For large volumes and small temperatures this is impossible in practice.

In the meron-cluster approach one solves the sign problem in two steps. In the first step one analytically re-writes the partition function using new variables such that it is possible to exactly cancel all negative weight configurations with configurations of positive weights. This group of configurations then does not contribute to the partition function. The remaining configurations are guaranteed to be positive. Thus, in the new variables, one effectively obtains Boltzmann weights with $\mathrm{Sign} = 0, 1$. At this stage, despite the fact that all negative signs have been eliminated, only one half of the sign problem has been solved since an algorithm that naively generates configurations with $\mathrm{Sign} = 0$ or 1 generates an exponentially large number of zero weight configurations. Thus, it is important to introduce a second step in which one avoids configurations that have been canceled analytically. In practice it is often useful to allow these zero-weight configurations to occur in a controlled manner since these configurations may contribute to observables. In a numerical algorithm a local Metropolis decision ensures that contributions of 0 and 1 occur with similar probabilities. This solves the sign problem completely.

1.2 The Meron-Cluster Method

The central idea behind the meron-cluster method is to express the partition function, which is originally written as a sum over weights of fermion occupation number configurations, as a sum over weights of configurations which contain both fermions and new bond variables. Mathematically this means

$$Z_f = \sum_{[n]} \mathrm{Sign}[n] \exp(-S[n]) = \sum_{[n,b]} \mathrm{Sign}[n,b] \exp(-S[n,b]) \tag{1.6}$$

where the bond variables b carry information about whether two lattice sites are connected or not. A cluster is defined as a set of connected lattice sites whose flip exchanges occupied and empty sites, i.e., the occupied sites on that cluster are emptied and the originally empty sites now become occupied. This step of re-writing the partition function is well known and has been used in earlier attempts of constructing fermion cluster algorithms as discussed in [8] and [9]. The recent progress results from the observation that the sign problem contained in a partition function of the form (1.6) is completely solvable if the magnitude $W[n,b]$ and the sign $\mathrm{Sign}[n,b]$ of the Boltzmann weight satisfy three requirements:

1. The magnitude of the Boltzmann weight $\exp(-S[n,b])$ does not change when any cluster is flipped.

2. The effect of a cluster-flip on the sign of the Boltzmann weight $\mathrm{Sign}[n,b]$ is independent of the orientation of all other clusters.

3. Starting from any configuration $[n,b]$, it must be possible to flip clusters and reach a *reference* configuration $[n_{\mathrm{ref}},b]$, which is guaranteed to have a positive Boltzmann weight.

In addition, a formula for the change in the sign of a configuration due to a cluster-flip has been derived recently [10]. Using this formula and other tricks it is usually possible to satisfy the first two properties for any given model. Restrictions in the class of solvable models arise due to the inability to satisfy the third property listed above, i.e., the existence of a reference configuration. However, we have been able to construct useful reference configurations for a variety of models.

The essential consequence of the three basic properties necessary for the meron-cluster approach to work is that clusters can be characterized by their effect on the sign. Clusters whose flip changes the sign are referred to as merons. Clearly a configuration with a meron-cluster contributes zero to the partition function after a partial re-summation over cluster-flips is performed[1]. All configurations without any merons contribute positively to the partition function. Thus the partition function can be

[1] This partial re-summation over cluster-flips is often referred to as an improved estimator.

re-written in terms of positive semi-definite Boltzmann weights, i.e., Sign $= 0, 1$. In order to avoid the zero-weight configurations, a re-weighting method that eliminates configurations containing multiple meron-clusters is included. In order to perform this re-weighting, all observables must also be measured using improved estimators. Fortunately, this is possible for most quantities of physical interest. Usually, physically interesting observables receive non-zero contributions also from configurations containing merons. For example, vacuum condensates receive contributions from the one-meron sector whereas observables derived from certain two-point correlation functions receive contributions from zero- and two-meron configurations only. Four-point correlation functions also receive non-zero contributions from four-meron configurations. Fortunately, one is usually not interested in multi-point correlation functions and for most purposes one can completely eliminate the configurations with more than two merons. This is exactly what happens in the re-weighting step of the meron-cluster algorithm. In this paper we do not discuss the re-weighting step although this is an essential part of the complete solution of the sign problem. We assume that once all negative signs are eliminated, one can design a re-weighting step that does not generate exponentially long auto-correlation times.

Although the three requirements for solving the sign problem with the meron-cluster method are somewhat restrictive, a large class of Hamiltonians for strongly interacting fermions is consistent with them. For example, in the case of spinless fermions it is necessary to include a certain amount of nearest-neighbor fermion repulsion [2] or a large chemical potential [3] depending on the hopping term. As we will see, similar restrictions arise for fermions with spin. In particular, the standard Hubbard model Hamiltonian cannot be treated with our method, while slightly modified models in the Hubbard model family can. In this paper we construct a large class of $SU(2)$ spin symmetric Hamiltonians for spin one-half fermions with nearest-neighbor interactions to which the meron-cluster method can be applied. The numerical results for one such model related to s-wave superconductivity have been discussed elsewhere [11].

The meron-cluster idea was first developed for a bosonic model with a complex action — the 2-d $O(3)$ model at non-zero vacuum-angle θ [12]. The term meron was introduced first to denote half-instantons. Indeed the meron-clusters in the 2-d $O(3)$ model are half-instantons [12]. The instanton number is the integer-valued topological charge $Q \in \mathbf{Z}$, which gives rise to a complex phase $\exp(i\theta Q)$ that contributes to the Boltzmann factor. At $\theta = \pi$ the phase factor reduces to a sign $\exp(i\pi Q) = (-1)^Q$, which distinguishes between sectors with even and odd topological charges. In the 2-d $O(3)$ model the meron-clusters carry half-integer topological charges. When such a cluster is flipped, its topological charge changes sign and hence the total topological charge of the configuration changes by an odd integer. Thus, the phase factor $(-1)^Q$ changes sign when a meron-cluster is flipped. Similarly, a meron-flip in the fermion cluster algorithm changes the sign of a fermion world-line configuration. Interestingly a $\mathbf{Z}(2)$ topological number can be assigned

to each fermionic configuration. Any configuration with Sign = 1 is topologically trivial because it represents an even permutation of fermions. A configuration with Sign = -1 is topologically distinct, because an odd permutation cannot be changed into an even one by a continuous deformation of fermion world-lines. In this sense, configurations with Sign = -1 are instantons. Flipping any meron changes the fermion sign and hence unwinds the instanton. In two spatial dimensions one can extend the analogy to the 2-d $O(3)$ model even further. Then particles can exist with any statistics, characterized by a parameter θ that varies between $\theta = 0$ for bosons and $\theta = \pi$ for fermions. For anyons the fermion sign is replaced by a complex phase factor $\exp(i\theta H)$, where $H \in Z$ is the integer-valued Hopf number. In that case the merons are half-Hopf-instantons.

The merons are not just of algorithmic interest. In fact, they are physical objects that allow us to understand the topology of the fermion world-lines and hence the origin of the fermion sign. The merons effectively bosonize a fermionic theory. When a fermionic model is formulated in terms of bosonic occupation numbers which interact locally, the fermion sign still induces non-local topological interactions. Hence, the resulting theory is not really bosonized. The merons, however, decompose the global topology of the fermion world-lines into manageable contributions that are local on the scale of the correlation length. This allows us to simulate fermions almost as efficiently as bosons.

1.3 Organization of the Paper

The paper is organized as follows. In section 2 the essential ideas behind the meron-cluster approach are illustrated for the simple case of spinless fermions. We discuss how the three properties necessary for the complete solution to the sign problem, discussed in section 1.2, place restrictions on the class of models that are solvable with the meron-cluster algorithm. In section 3 we build a class of models of fermions with spin which are solvable using meron-cluster methods. We also discuss improved estimators for some physical quantities useful for the study of superconductivity that receive contributions from zero- and two-meron configurations and present some data from a recent numerical simulation. We also show how one can extend these models by adding new terms to the Hamiltonian that appear to violate the properties necessary for the meron-cluster method to work but do not introduce sign problems. In particular, we show how a repulsive Hubbard model becomes solvable in the presence of a chemical potential. Section 4 contains a discussion of the efficiency of meron-cluster algorithms. Finally, in section 5 we end with some conclusions.

2 Meron-Cluster Solution for Spinless Fermions

Let us illustrate the essential steps that yield solutions to sign problems in the meron-cluster approach using the example of spinless fermions. This is essentially a combination of results first discussed in [2, 3] and [10]. This will serve as a preparation for the main subject of this paper — namely fermions with spin.

2.1 Fermion Path Integral in Fock State Basis

We consider fermions hopping on a d-dimensional cubic lattice of volume $V = L^d$ sites with periodic or anti-periodic spatial boundary conditions. The fermions are described by creation and annihilation operators $c_x^\dagger$ and c_x with standard anti-commutation relations

$$\{c_x^\dagger, c_y^\dagger\} = 0,\ \{c_x, c_y\} = 0,\ \{c_x^\dagger, c_y\} = \delta_{xy}. \tag{2.1}$$

Following Jordan and Wigner [13] we represent these operators by Pauli matrices

$$c_x^\dagger = \sigma_1^3\sigma_2^3...\sigma_{l-1}^3\sigma_l^+,\ c_x = \sigma_1^3\sigma_2^3...\sigma_{l-1}^3\sigma_l^-,\ n_x = c_x^\dagger c_x = \frac{1}{2}(\sigma_l^3 + 1), \tag{2.2}$$

where

$$\sigma_l^\pm = \frac{1}{2}(\sigma_l^1 \pm i\sigma_l^2),\ [\sigma_l^i, \sigma_m^j] = i\delta_{lm}\epsilon_{ijk}\sigma_l^k. \tag{2.3}$$

Here l labels the lattice point x. The Jordan-Wigner representation requires an ordering of the lattice points. For example, one can label the point $x = (x_1, x_2, ..., x_d)$ by $l = x_1 + x_2L + ... + x_dL^{d-1}$. It can be shown that the physics is completely independent of the ordering. Further, the Jordan-Wigner representation works in any dimension.

Instead of considering the most general model that can be solved using the meron-concept, we restrict ourselves to a class of Hamiltonians that conserve particle number. From the discussion below it will become clear how to extend the ideas presented here to other Hamiltonians while maintaining the ability to solve the associated sign problem. With this in mind we focus on a Hamilton operator of the form

$$H = \sum_{x,i} h_{x,i}, \tag{2.4}$$

which is a sum of nearest-neighbor Hamiltonians $h_{x,i}$ given by

$$h_{x,i} = -\frac{t}{2}(c_x^\dagger c_{x+\hat{i}} + c_{x+\hat{i}}^\dagger c_x) + U(n_x - \frac{1}{2})(n_{x+\hat{i}} - \frac{1}{2}). \tag{2.5}$$

which couples the fermion operators at the lattice sites x and $x + \hat{i}$, where $\hat{i}$ is a unit-vector in the i-direction. Next we decompose the Hamilton operator into $2d$ terms

$$H = H_1 + H_2 + ... + H_{2d}, \tag{2.6}$$

with

$$H_i = \sum_{\substack{x=(x_1,x_2,\ldots,x_d) \\ x_i \text{even}}} h_{x,i}, H_{i+d} = \sum_{\substack{x=(x_1,x_2,\ldots,x_d) \\ x_i \text{odd}}} h_{x,i}. \tag{2.7}$$

Note that the individual contributions to a given H_i commute with each other, but two different H_i do not commute. Using the Trotter-Suzuki formula we express the fermionic grand canonical partition function as

$$\begin{aligned} Z_f &= \mathrm{Tr}\{\exp[-\beta(H-\mu N)]\} \\ &= \lim_{M\to\infty} \mathrm{Tr}\left\{\exp[-\epsilon(H_1 - \frac{\mu}{2d}N)]\exp[-\epsilon(H_2 - \frac{\mu}{2d}N)]...\exp[-\epsilon(H_{2d} - \frac{\mu}{2d}N)]\right\}^M. \end{aligned} \tag{2.8}$$

Here $N = \sum_x n_x$ is the particle number operator and μ is the chemical potential. We have introduced M Euclidean time-slices with $\epsilon = \beta/M$ being the lattice spacing in the Euclidean time-direction. We insert complete sets of fermion Fock states between the factors $\exp[-\epsilon(H_i - \frac{\mu}{2d}N)]$. Each site is either empty or occupied, i.e. n_x has eigenvalue 0 or 1. In the Jordan-Wigner representation this corresponds to eigenstates $|0\rangle$ and $|1\rangle$ of σ_l^3 with $\sigma_l^3|0\rangle = -|0\rangle$ and $\sigma_l^3|1\rangle = |1\rangle$. The transfer matrix is a product of factors

$$\begin{aligned} &\exp[-\epsilon(h_{x,i} - \frac{\mu}{2d}(n_x + n_{x+\hat{i}}))] = \exp[\epsilon(\frac{U}{4} + \frac{\mu}{2d})] \\ &\times \begin{pmatrix} \exp[-\epsilon(\frac{U}{2} + \frac{\mu}{2d})] & 0 & 0 & 0 \\ 0 & \cosh(\frac{\epsilon t}{2}) & \Sigma\sinh(\frac{\epsilon t}{2}) & 0 \\ 0 & \Sigma\sinh(\frac{\epsilon t}{2}) & \cosh(\frac{\epsilon t}{2}) & 0 \\ 0 & 0 & 0 & \exp[-\epsilon(\frac{U}{2} - \frac{\mu}{2d})] \end{pmatrix}, \end{aligned} \tag{2.9}$$

which is a 4×4 matrix in the Fock space basis $|00\rangle$, $|01\rangle$, $|10\rangle$ and $|11\rangle$ of two sites x and $x + \hat{i}$. Here $\Sigma = \sigma_{l+1}^3\sigma_{l+2}^3...\sigma_{m-1}^3$ is a string of Pauli matrices running over consecutive labels between l and m, where l is the smaller of the labels for the lattice points x and $x + \hat{i}$ and m is the larger label. Note that Σ is diagonal in the occupation number basis.

The partition function is now expressed as a path integral

$$Z_f = \sum_{[n]} \mathrm{Sign}[n]\exp(-S[n]), \tag{2.10}$$

over configurations of occupation numbers $n(x,t) = 0, 1$ on a $(d+1)$-dimensional space-time lattice of points (x,t). The magnitude of the Boltzmann factor,

$$\begin{aligned} &\exp(-S[n]) = \\ &\prod_{p=0}^{M-1}\prod_{i=1}^{d} \prod_{\substack{x=(x_1,x_2,\ldots,x_d) \\ x_i\text{even, t=2dp+i-1}}} \exp\{-s[n(x,t), n(x+\hat{i},t), n(x,t+1), n(x+\hat{i},t+1)]\} \\ &\times \prod_{\substack{x=(x_1,x_2,\ldots,x_d) \\ x_i\text{odd, t=2dp+d+i-1}}} \exp\{-s[n(x,t), n(x+\hat{i},t), n(x,t+1), n(x+\hat{i},t+1)]\}, \end{aligned} \tag{2.11}$$

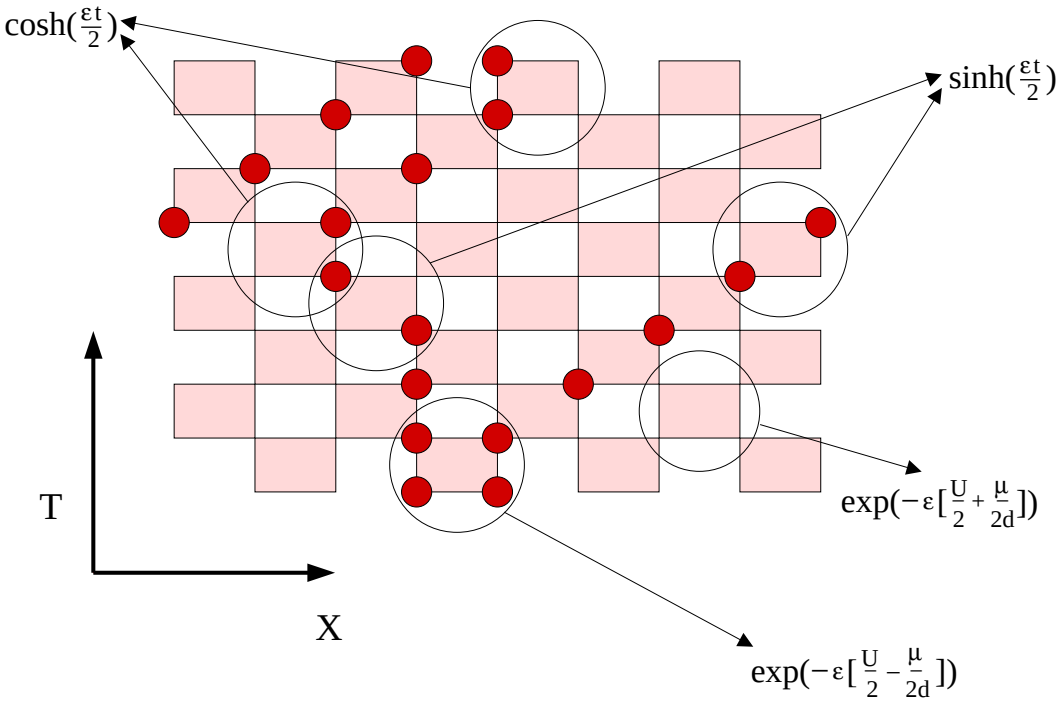

Figure 1: *A typical fermion world-line configuration in one spatial dimension with periodic boundary conditions. The product of* Σ *factors from each plaquette is negative for this configuration since the two fermions exchange their positions with each other.*

is a product of space-time plaquette contributions with

$$\begin{aligned}
&\exp(-s[0,0,0,0]) = \exp[-\epsilon(\frac{U}{2}+\frac{\mu}{2d})],\\
&\exp(-s[0,1,0,1]) = \exp(-s[1,0,1,0]) = \cosh(\frac{\epsilon t}{2}),\\
&\exp(-s[0,1,1,0]) = \exp(-s[1,0,0,1]) = \sinh(\frac{\epsilon t}{2}),\\
&\exp(-s[1,1,1,1]) = \exp[-\epsilon(\frac{U}{2}-\frac{\mu}{2d})].
\end{aligned} \tag{2.12}$$

All the other Boltzmann factors are zero, which implies several constraints on allowed configurations. Note that we have dropped the trivial overall factor $\exp[\epsilon(\frac{U}{4}+\frac{\mu}{2d})]$ in eq.(2.9). The sign of the Boltzmann factor Sign$[n]$ also is a product of space-time plaquette contributions $\mathrm{sign}[n(x,t), n(x+\hat{i},t), n(x,t+1), n(x+\hat{i},t+1)]$ with

$$\begin{aligned}
&\mathrm{sign}[0,0,0,0] = \mathrm{sign}[0,1,0,1] = \mathrm{sign}[1,0,1,0] = \mathrm{sign}[1,1,1,1] = 1,\\
&\mathrm{sign}[0,1,1,0] = \mathrm{sign}[1,0,0,1] = \Sigma.
\end{aligned} \tag{2.13}$$

It should be noted that the non-local string of Pauli matrices Σ gets contributions from all lattice points with labels between l and m. This would make an evaluation

of the fermion sign rather tedious. Also, it is not a priori obvious that Sign$[n]$ is independent of the arbitrarily chosen order of the lattice points. Fortunately, there is a simple way to compute Sign$[n]$ which is directly related to the Pauli principle and which is manifestly order-independent. In fact, Sign$[n]$ has a topological meaning. The occupied lattice sites define fermion world-lines which are closed around the Euclidean time-direction. Of course, during their Euclidean time-evolution fermions can interchange their positions, and the fermion world-lines define a permutation of particles. The Pauli principle dictates that the fermion sign is just the sign of that permutation. When one works with anti-periodic spatial boundary conditions, Sign$[n]$ receives an extra minus-sign for every fermion world-line that crosses the boundary. Figure 1 shows a typical configuration in one spatial dimension along with examples of contributions to the Boltzmann weight arising from local space-time plaquettes.

2.2 Observables in Fermionic Fock Space

A variety of observables of physical interest take on a simple form in Fock space. Typically the expectation value of an operator O is given by

$$\langle O \rangle_f = \frac{1}{Z_f} \sum_{[n]} O[n] \mathrm{Sign}[n] \exp(-S[n]). \tag{2.14}$$

For example, the total particle number relative to half-filling

$$N[n] - \frac{V}{2} = \sum_x \left(n(x,t) - \frac{1}{2} \right), \tag{2.15}$$

which is conserved and hence the same in each time-slice, and its disconnected susceptibility

$$\chi_N = \frac{\beta}{V} \left\langle \left(N - \frac{V}{2} \right)^2 \right\rangle_f \tag{2.16}$$

are both operators that are diagonal in the occupation number basis. Other quantities of physical interest are the staggered occupation

$$O[n] = \epsilon \sum_{x,t} (-1)^{x_1+x_2+\ldots+x_d} \left(n(x,t) - \frac{1}{2} \right), \tag{2.17}$$

and the corresponding susceptibility

$$\chi_O = \frac{1}{\beta V} \left(\langle O^2 \rangle_f - \langle O \rangle_f^2 \right). \tag{2.18}$$

We can also measure the winding number $W_i[n]$ around the spatial direction i

$$W_i[n] \;=\; \sum_{p=0}^{M-1} \sum_{\substack{x=(x_1,x_2,\ldots,x_d) \\ x_i \mathrm{even},\ \mathrm{t=2dp+i-1}}} \frac{1}{L} \left\{ \delta_{[n(x,t),n(x+\hat{i},t),n(x,t+1),n(x+\hat{i},t+1)],[1,0,0,1]} \right.$$

$$- \delta_{[n(x,t),n(x+\hat{i},t),n(x,t+1),n(x+\hat{i},t+1)],[0,1,1,0]}\Big\}$$

$$+ \sum_{\substack{x=(x_1,x_2,\ldots,x_d) \\ x_i \text{odd, t=2dp+d+i-1}}} \frac{1}{L}\Big\{\delta_{[n(x,t),n(x+\hat{i},t),n(x,t+1),n(x+\hat{i},t+1)],[1,0,0,1]}$$

$$- \delta_{[n(x,t),n(x+\hat{i},t),n(x,t+1),n(x+\hat{i},t+1)],[0,1,1,0]}\Big\}. \quad (2.19)$$

This counts 1 for a plaquette configuration $[1,0,0,1]$, i.e., for a fermion hopping in the positive i-direction, and -1 for $[0,1,1,0]$, i.e., for a fermion hopping in the opposite direction. As a result, $W_i[n]$ counts how many fermions wrap around the i-direction during their Euclidean time-evolution. Again, one can define a corresponding susceptibility

$$\chi_{W_i} = \beta \langle W_i^2 \rangle_f. \quad (2.20)$$

We will use a similar quantity as an order parameter for superconductivity in models of fermions with spin. It measures the response of the system to a twist in the spatial boundary conditions. In the infinite volume limit the system feels the spatial boundary only in a phase with long-range correlations.

Observables like the two-point Green function defined by

$$G(x,t;y,t') = \frac{\text{Tr}\left\{\exp\left[-(\beta-t)H\right] c_x \exp\left[-(t-t')H\right] c_y^\dagger \exp\left[-t'H\right]\right\}}{\text{Tr}\left\{\exp\left[-\beta H\right]\right\}} \quad (2.21)$$

are quite useful to extract the spectral information of H. These expectation values of non-diagonal operators can also be obtained like those of the diagonal operators using

$$G(x,t;y,t') = \frac{1}{Z_f} \sum_{[n']} \text{Sign}[n'] \exp(-S[n']). \quad (2.22)$$

where the configurations $[n']$ that contribute are different from the configurations that contribute to the partition function due to the violation of fermion number at the space-time sites (x,t) and (y,t'). In order to allow for these violations it is convenient to introduce two new time-slices at t and t'. The factors $\exp(-S[n'])$ and $\text{Sign}[n']$ can be calculated in the same way as before on all the time-slices except on the two slices where fermionic creation and annihilation operators are introduced. At those two slices the fermion occupation number changes appropriately and the Jordan-Wigner representation can be used to figure out the extra sign factor coming from the string of σ_3 associated with fermionic creation and annihilation operators. Interestingly, as discussed in [14], once the path integral is re-written in terms of cluster variables, it is straightforward to keep track of these new configurations along with the configurations that contribute to the path integral and hence such observables can also be measured.

2.3 Cluster Decomposition of the Partition Function

Up to now we have derived a path integral representation for the fermion system in terms of bosonic occupation numbers and a fermion sign factor that encodes Fermi statistics. The system without the sign factor is bosonic and is characterized by the positive Boltzmann factor $\exp(-S[n])$. Here the bosonic model turns out to be a quantum spin system with the Hamiltonian

$$H = \sum_{x,i} [t(S^1_x S^1_{x+\hat{i}} + S^2_x S^2_{x+\hat{i}}) + U S^3_x S^3_{x+\hat{i}}] - \mu \sum_x S^3_x, \tag{2.23}$$

where $S^i_x = \frac{1}{2}\sigma^i_l$ is a spin 1/2 operator associated with the lattice site x that was labeled by l. The case $U = t$ corresponds to the isotropic anti-ferromagnetic quantum Heisenberg model, while $U = 0$ represents the quantum XY-model. The chemical potential plays the role of an external magnetic field.

It is well known that the partition function for the above quantum spin model can be re-written in terms of cluster variables. This cluster representation is at the heart of the the loop-cluster algorithm [15, 16] that is used to simulate the quantum spin model very efficiently. Interestingly, the meron-cluster algorithm for the fermionic model is also based on a similar cluster decomposition of the partition function. The essential differences come from the fermion sign factor and are encoded in the topology of the clusters. Once the connection between the fermion permutation sign and the topology of the clusters is understood, the cluster algorithm for the quantum spin system can be modified easily to deal with the fermionic model.

Let us first discuss the essential steps in the cluster decomposition of the partition function of the quantum spin model. The main idea is to take a configuration of quantum spins and re-write the weight as a sum over weights of configurations with spins and bonds, such that the magnitude of the weight of the configuration does not change when the set of spins connected by bonds are flipped. For the problem at hand this decomposition can be accomplished at every plaquette. For example, the Boltzmann weights of each plaquette given in eq.(2.12) can be written as

$$\begin{aligned} &\exp(-s[n(x,t), n(x+\hat{i},t), n(x,t+1), n(x+\hat{i},t+1)]) = \\ &\quad \sum_{b=A,B,C,D} \exp\left(-s[n(x,t), n(x+\hat{i},t), n(x,t+1), n(x+\hat{i},t+1); b]\right), \end{aligned} \tag{2.24}$$

where $b = A, B, C, D$ represent four types of bond break-ups. The Boltzmann weights $\exp(-s[n; b])$ can be arbitrary as long as they satisfy eq.(2.24). Here we choose

$$\begin{aligned} &\exp(-s[0,0,0,0;A]) = \exp(-s[1,0,1,0;A]) = \exp(-s[0,1,0,1;A]) = \\ &\quad \exp(-s[1,1,1,1;A]) = W_A = \frac{1}{2}\left\{\exp\left(-\epsilon\left[\frac{U}{2} + \frac{\mu}{2d}\right]\right) + \exp\left(-\frac{\epsilon t}{2}\right)\right\}, \\ &\exp(-s[0,0,0,0;B]) = \exp(-s[1,0,0,1;B]) = \exp(-s[0,1,1,0;B]) = \end{aligned}$$

$$
\begin{aligned}
-\exp\left(-s[1,1,1,1;B]\right) \;&=\; W_B \;=\; -\exp\left(-\frac{\epsilon U}{2}\right)\,\sinh\left(\frac{\epsilon\mu}{2d}\right), \\
\exp\left(-s[0,0,0,0;C]\right) \;&=\; \exp\left(-s[1,0,0,1;C]\right) \;=\; \exp\left(-s[0,1,1,0;C]\right) \;= \\
&\exp\left(-s[1,1,1,1;C]\right) \;=\; W_C \;=\; \frac{1}{2}\left\{\exp\left(-\epsilon\left[\frac{U}{2}-\frac{\mu}{2d}\right]\right)-\exp\left(-\frac{\epsilon t}{2}\right)\right\}, \\
\exp\left(-s[1,0,1,0;D]\right) \;&=\; \exp\left(-s[0,1,0,1;D]\right) \;=\; \exp\left(-s[0,1,1,0;D]\right) \;= \\
&\exp\left(-s[1,0,0,1;D]\right) \;=\; W_D \;=\; \frac{1}{2}\left\{\exp\left(\frac{\epsilon t}{2}\right)-\exp\left(-\epsilon\left[\frac{U}{2}+\frac{\mu}{2d}\right]\right)\right\}.
\end{aligned}
\tag{2.25}
$$

to be the only non-zero weights. The above equations are shown pictorially in figure 2. If we interpret the spin states as fermion occupation numbers, clearly $W[n,b]$ satisfies the first property discussed in section 1.2. We will now assume that $\mu \leq 0$ and $t + \mu/d \geq U$, so that all the Boltzmann weights $\exp(-s[n;b])$ of spin and bond configurations are positive. However, notice that there is an extra negative sign for each plaquette with configuration $[1,1,1,1;B]$. Such negative signs must be considered separately as a contribution to the sign of a given spin and bond configuration. Explicitly this is given by $(-1)^{N_B}$ where N_B is the number of plaquettes of the type $[1,1,1,1;B]$. Generally, such extra sign factors must be avoided since they can lead to sign problems. However, since we anyway have to deal with the non-local fermion signs, which we have suppressed until now, we will allow for such extra negative sign factors. As we will see below, these local sign factors can sometimes be helpful in canceling sign factors that arise due to fermion permutations.

Based on the decomposition given in eq.(2.24) the original partition function of the fermionic model can be written as

$$
Z_f = \sum_{[n,b]} \mathrm{Sign}[n,b]\;\exp(-S[n,b]), \tag{2.26}
$$

a sum over configurations of occupation numbers $n(x,t) = 0, 1$ and bond variables $b = A, B, C, D$ on each plaquette. The sign $\mathrm{Sign}[n,b]$ is the product of the original fermion permutation sign due to the occupation numbers and $(-1)^{N_B}$. The new configurations naturally connect neighboring sites through the bonds that live on each individual space-time interaction plaquette as represented pictorially in figure 2. A sequence of connected sites defines a cluster. Since each bond on a plaquette connects two sites, every cluster is a simple closed loop. Thus we have written the partition function of a fermionic model in terms of the statistical mechanics of closed interacting loops with not necessarily positive Boltzmann weights. Although we have illustrated this using a particular model, it is straightforward to repeat the above steps for any model. When a cluster is flipped, the occupation numbers of all the sites on the cluster are changed from $n(x,t)$ to $1 - n(x,t)$. In other words, a cluster-flip interchanges occupied and empty sites. The weights given in eq.(2.25) guarantee that the magnitude of the weight of a configuration does not change when

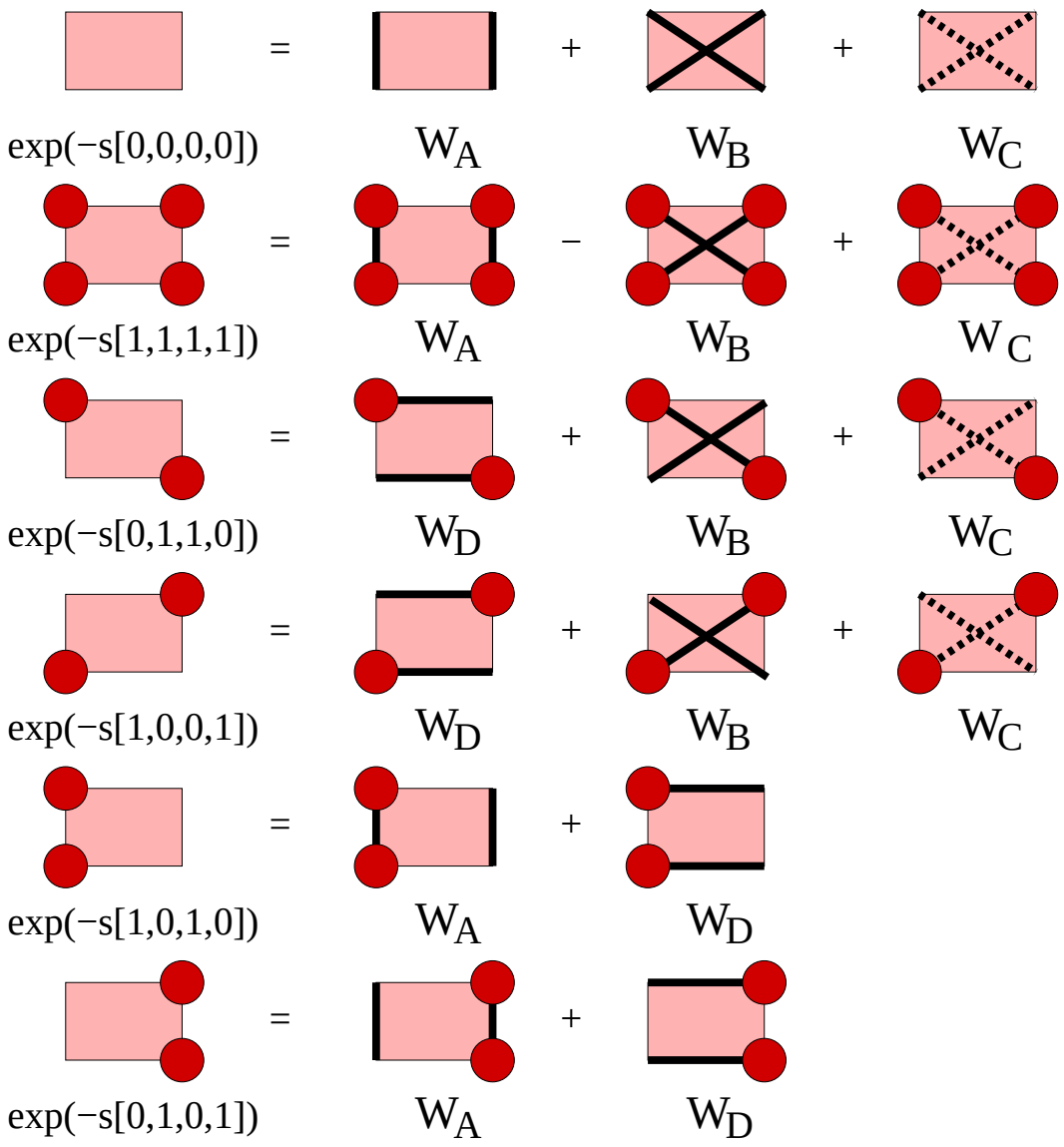

Figure 2: *The pictorial representation of the decomposition of plaquette weights of fermion occupation number configurations in terms of weights of bonds and fermion occupation numbers.*

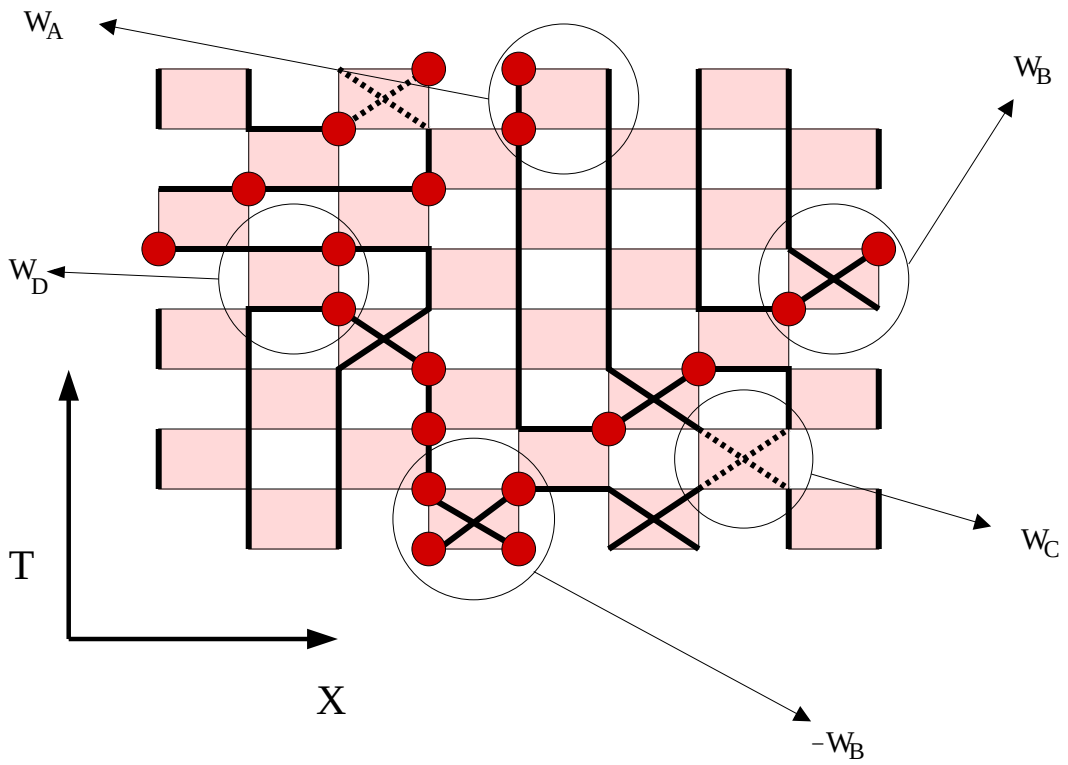

Figure 3: *A typical configuration of fermion occupation numbers and bonds in one spatial dimension.*

a cluster is flipped. A typical configuration in one spatial dimension is represented schematically in figure 3.

2.4 Meron-Clusters and Reference Configurations

Let us now consider the effect of a cluster-flip on the sign factor. In the example considered, the sign of a given configuration of spins and bonds arises from two factors. One is the permutation of fermion world-lines which is independent of the bond configuration and the other is due to plaquettes of type $[1, 1, 1, 1; B]$ each of which contributes a negative sign to the Boltzmann weight. Obviously, a cluster-flip either changes the sign of a configuration or not. In general, the effect of the flip of a specific cluster on the fermion sign depends on the orientation of the other clusters. For example, a cluster whose flip does not change the sign now, may very well change the sign after other clusters have been flipped. In other words, in general the clusters affect each other in their effect on the configuration's sign. Recently, a formula for how cluster-flips affect the fermion permutation sign was discovered [10]. The relevant information is encoded by an integer which can be determined by starting at an arbitrary point on the loop-cluster and traversing around it in

either direction and flipping the sites as they are encountered. As we go around the loop, we denote the number of horizontal bonds (D-type bonds) encountered while entering an occupied site from an empty site (before they are flipped) by N_h, the number of cross-bonds (B- or C-type bonds) traversed while the other cross-bond on the same plaquette connects two occupied sites by N_x, and the temporal winding of the cluster by N_w. Then the cluster-flip changes the fermion permutation sign if and only if

$$N = N_h + N_w + N_x \tag{2.27}$$

is even. For details of how this can be derived we refer the reader to [10]. A similar formula can be derived for the signs associated with the plaquettes of the type $[1, 1, 1, 1; B]$. In this case, again as we traverse the loop-cluster and flip the sites, if N_{xB} is the number of B-type cross-bonds encountered when the other cross-bond connects two occupied sites, then the cluster-flip changes the sign associated with the plaquettes of the type $[1, 1, 1, 1; B]$ if N_{xB} is odd. Using this formula we discover that in the present model the effect of a cluster-flip on the sign of a configuration in general depends on the orientation of other clusters. In particular, if two clusters cross each other in an odd number of C-type cross-bonds then the flip of one cluster has an effect on whether the other cluster-flip changes the configuration sign or not. Interestingly, once we forbid C-type cluster break-ups, i.e. when $W_C = 0$, the clusters have a remarkable property with far reaching consequences: each cluster can be characterized by its effect on the fermion sign independent of the orientation of all the other clusters. We refer to clusters whose flip changes $\mathrm{Sign}[n, b]$ as merons, while clusters whose flip leaves $\mathrm{Sign}[n, b]$ unchanged are called non-merons. The flip of a meron-cluster permutes the fermions and changes the topology of the fermion world-lines. Notice that the B-type cross-bonds are still allowed thanks to the extra negative signs that arise due to signs from $[1, 1, 1, 1; B]$ plaquettes. Thus we have been able to ensure the first two properties discussed in section 1.2, provided we satisfy the constraints $\mu \leq 0$, $t + \mu/d \geq U$ and $W_C = 0$ which implies $t = U - \mu/d$.

When the cluster-flips affect the sign factor independently, it is easy to average analytically over all the cluster-flips. Such an average over cluster-flips for a given bond configuration is referred to as an improved estimator in the language of cluster algorithms. We will discuss improved estimators of some observables in the next section. Averaging the sign over cluster-flips, the fermionic partition function can be re-written as

$$Z_f = \sum_{[n,b]} \overline{\mathrm{Sign}[b]}\ \exp(-S[n, b]), \tag{2.28}$$

where

$$\overline{\mathrm{Sign}[b]}\ =\ \frac{1}{2^{N_C}} \sum_{\mathrm{cluster-flips}} \mathrm{Sign}[n, b]. \tag{2.29}$$

Thus $\overline{\mathrm{Sign}[b]} = 0$ if at least one of the clusters is a meron. In order to solve the sign problem it is important to eliminate configurations with meron-clusters from the Monte Carlo sampling. Unfortunately, this alone does not guarantee that the

contributions from the zero-meron sector will always be positive, although it may alleviate the sign problem considerably. With no merons in the configuration it is clear that the sign of a configuration remains unchanged under cluster-flips, but one could still have $\mathrm{Sign}[n, b] = -1$. In order to solve the sign problem completely it is necessary to show that configurations with no merons are always positive. This takes us to the third property discussed in section 1.2, the need for a reference configuration with a positive weight. Interestingly, there exists a class of models where this is achievable. It is then easy to show that $\overline{\mathrm{Sign}[b]} = 1$ in the non-meron sector. This solves the sign problem completely. Thus the fermionic partition function is obtained as a sum over weights of configurations in the zero-meron sector,

$$Z_f = \sum_{[b],\mathrm{zero-meron}} 2^{N_c} W[b], \tag{2.30}$$

where $W[b]$ is obtained as a product of local weights W_A, W_B and W_D.

There are at least two types of reference configurations that arise for spinless fermions. For example, in addition to setting $W_C = 0$, if we eliminate the B-type bonds completely by also setting $W_B = 0$, the remaining cluster break-ups have a remarkable property. They guarantee that sites inside a cluster obey a pattern of staggered occupation, i.e. either the even sites (with $x_1 + x_2 + ... + x_d$ even) within the cluster are all occupied and the odd sites are all empty or vice versa. This guarantees that the clusters can be flipped such that one reaches the totally staggered configuration in which all even sites at every time-slice are occupied and all odd sites are empty. In this half-filled configuration all fermions are static, no fermions are permuted during the Euclidean time-evolution. Further, since the model has no other sign factors, we know that $\mathrm{Sign}[n_{\mathrm{ref}}, b] = 1$. Since any configuration can be turned into the totally staggered configuration by appropriate cluster-flips, property three is indeed satisfied. The condition $W_B = 0$ and $W_C = 0$ leads to the restriction $\mu = 0$ and $t = U$. This leads to an interesting interacting spinless fermion model. A variant of this model has been studied in [2, 5, 6, 7] where it has been shown that the model can be used to study the spontaneous breaking of a $\mathbf{Z}(2)$ symmetry.

The second reference configuration is obtained by setting $W_D = 0$ along with $W_C = 0$. In this case we see that all sites in a given cluster have the same occupation number, i.e., all are either empty or all are occupied. This means that all clusters can be flipped such that one reaches a configuration where all sites are empty. Since there are no fermions at all, there is no fermion permutation sign in this configuration. Further, there are no negative signs because of plaquettes of the form $[1, 1, 1, 1; B]$, since all sites are empty and $[0, 0, 0, 0; B]$ is positive. Therefore the configurations with no merons necessarily have a positive sign. The condition $W_C = 0$ and $W_D = 0$ leads to the restriction $U = 0$ and $t = -\mu/d$ with $\mu \leq 0$. This model leads to free non-relativistic fermions and has been discussed in [3].

Figure 4 shows a typical configuration and the associated reference configuration for each of the two classes discussed above. The reference configurations are closely

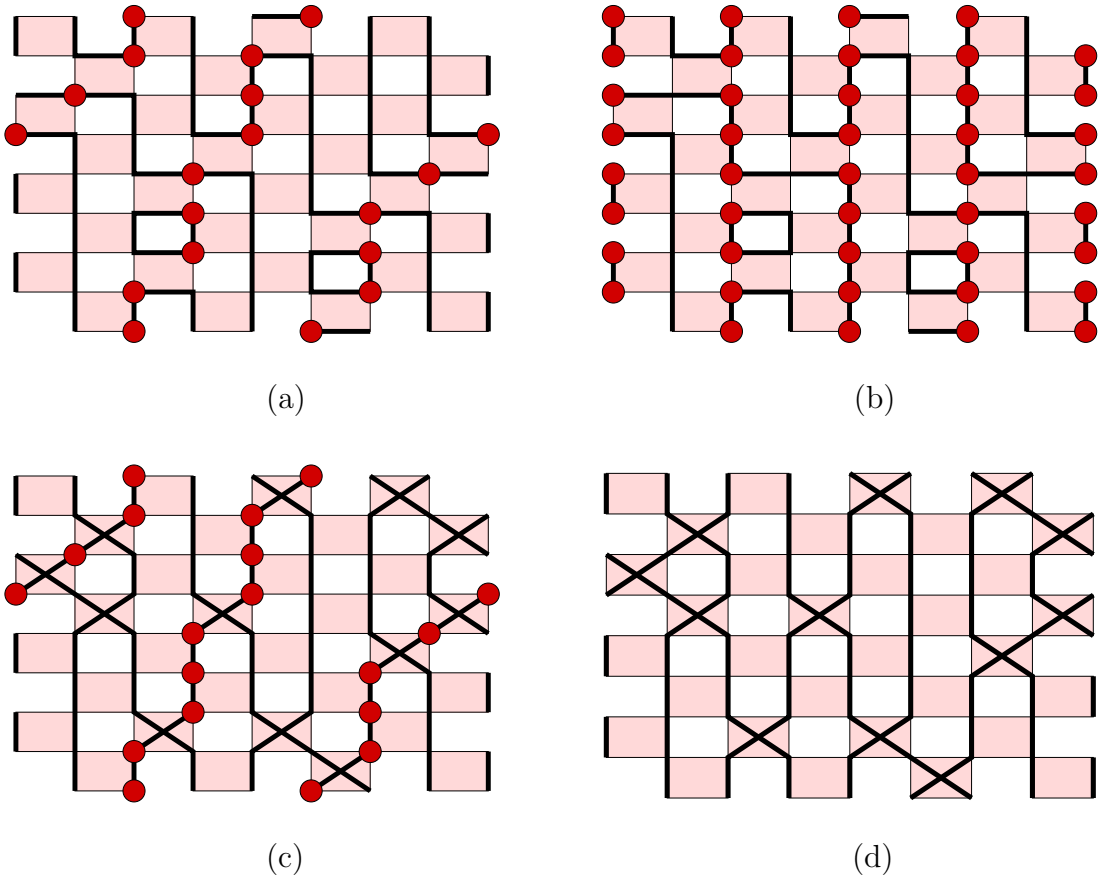

Figure 4: *Figure (a) shows a typical fermion and bond configuration without cross-bonds and (b) shows the corresponding reference configuration which has a positive sign. Figures (c) and (d) show similar configurations for the case without horizontal bonds.*

connected with the ground state properties of each model. The staggered reference configuration naturally describes theories with spontaneously broken ground states whereas the totally empty configuration leads to free non-relativistic fermions. It is possible to include a limited form of additional interactions without destroying any of the useful properties in these two classes of theories. However, it would be interesting to find new reference configurations which can lead to interesting physics. Of course, there are a variety of non-translationally invariant reference configurations which could describe electronic properties of certain crystalline structures. These models may be worth exploring. As we will show below, novel reference configurations also arise when spin is introduced.

2.5 Building-Blocks of Cluster Models

The results of the last two sections can be used to synthesize simple rules that help in building models of spinless fermions which automatically satisfy the first two properties of the meron-cluster approach, i.e. the weight of a configuration of clusters does not change under a cluster-flip and the effect on the sign of a configuration due to a cluster-flip is independent of all other clusters. In the models constructed above we started with four types of bond interactions namely the A-, B-, C- and D-types as shown in the figure 5. Each of these interactions can be associated with an operator acting on the two-site Hilbert space. For example, a plaquette with A-type (vertical) bonds gives the same positive weight to all diagonal elements. Hence A-type bonds are equivalent to the unit matrix. Similarly, the B-, C- and D-type bonds are equivalent to operators tabulated in table 1. The fermionic nature of the creation and annihilation operators are encoded in the formula of eq.(2.27) which is used to figure out the relative sign of configurations when clusters are flipped. Using eq.(2.27) along with the weights of the building-blocks, we found that

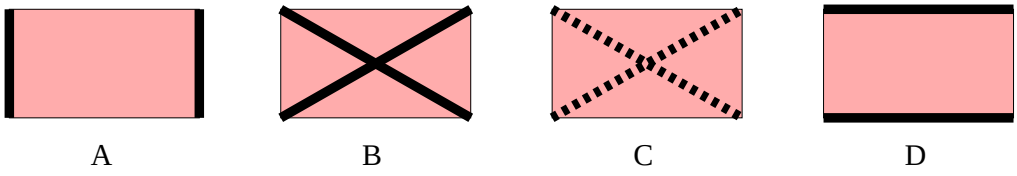

Figure 5: *Building-blocks of the two-site interactions discussed in the text.*

Bond-type	Transfer Matrix
A	$\mathbf{1}$
B	$c_x^\dagger c_y + c_y^\dagger c_x - n_x - n_y + 1$
C	$c_x^\dagger c_y + c_y^\dagger c_x + 2(n_x - 1/2)(n_y - 1/2) + 1/2$
D	$c_x^\dagger c_y + c_y^\dagger c_x - 2(n_x - 1/2)(n_y - 1/2) + 1/2$

Table 1: *The two-site building-blocks of figure 5 and their transfer matrix contributions.*

type C bonds are forbidden as they violate the required property that cluster-flips should have an independent effect on the sign. Thus the A-, B- and D-type bonds provide the basic building-blocks for constructing Hamiltonians which satisfy the two necessary requirements of the meron-cluster approach. We only need to ensure the existence of a reference configuration. This restriction then forbids models which simultaneously allow B- and D-type bonds. Thus, we find two types of solvable models discussed above. It is easy to construct the Hamiltonian of these models using the corresponding building blocks. For example, the model with A- and B-type bonds leads to the two-site transfer matrix $T_{xy} = W_A + W_B[c_x^\dagger c_y + c_y^\dagger c_x - n_x - n_y + 1]$,

which in the limit $\epsilon \to 0$ yields $T_{xy} = 1 + \epsilon[c_x^\dagger c_y + c_y^\dagger c_x - n_x - n_y + 1]$. Since all two-site interactions contribute equally to the full Hamiltonian, $H = \sum_{<xy>} h_{xy}$, in this limit we can identify $T = 1 - \epsilon H$, which yields

$$h_{xy} = -(c_x^\dagger c_y + c_y^\dagger c_x) + n_x + n_y \tag{2.31}$$

up to additive and multiplicative constants. Similarly the model obtained with A- and D-type bonds leads to

$$h_{xy} = -(c_x^\dagger c_y + c_y^\dagger c_x) + 2(n_x - 1/2)(n_y - 1/2). \tag{2.32}$$

Thus, one can construct the Hamilton operator once the building-blocks are chosen in terms of the bond break-ups on an elementary plaquette. Later, we will use this procedure to construct models of fermions with spin. In eq. (2.31) and eq. (2.32) we have chosen to normalize the hopping term and set $t = 1$. In the remainder of this article we will continue to adopt this normalization for convinence.

2.6 Improved Estimators

Based on the previous discussion it is clear that the partition function can be written entirely in terms of cluster variables as

$$Z_f \;=\; \sum_{[b],\mathrm{zero-meron}} 2^{N_C}\; W[b] \tag{2.33}$$

where N_C is the total number of clusters and the sum is over cluster configurations without meron-clusters. Similarly, it is possible to find expressions for observables in the language of clusters. For example, consider the deviation of the average occupation number of a configuration from half-filling which is defined as

$$\Delta n \;=\; n - \frac{1}{2} = \frac{1}{V}\sum_x \left(n_x - \frac{1}{2}\right). \tag{2.34}$$

Clearly it must be possible to sum over x belonging to a particular cluster $\mathcal{C} \in [b]$ first and then sum over all possible clusters. If we define

$$\Omega_{\mathcal{C}} = \sum_{x\in\mathcal{C}} (n_x - 1/2), \tag{2.35}$$

it is easy to see that $\Delta n = (1/V)\sum_{\mathcal{C}} \Omega_{\mathcal{C}}$. Performing a partial average over flips of fermionic occupation numbers belonging to various clusters one finds that this average is non-zero only in the one-meron sector and in this sector

$$\langle \Delta n \rangle_{\mathrm{cluster-flips}} \;=\; \frac{1}{V}\,\Omega_{\mathcal{C}_{\mathrm{meron}}} \tag{2.36}$$

where $\Omega_{\mathcal{C}_{\rm meron}}$ is to be calculated for the meron-cluster which is flipped into the reference configuration. Thus the complete answer turns out to be

$$\langle \Delta n \rangle = \frac{1}{Z_f} \sum_{[b],\text{one-meron}} \frac{\Omega_{\mathcal{C}_{\rm meron}}}{V} 2^{N_C} W[b]. \tag{2.37}$$

In the case of spinless fermion models discussed above, it is easy to see that $\Omega_{\mathcal{C}}$ is equal to the temporal winding of the cluster $\mathcal{C}$ up to a factor of 2. For the model described by the Hamiltonian of eq.(2.32), $\langle \Delta n \rangle = 0$ since there is no contribution from the single-meron sector to the partition function. Similar improved estimators for the chiral condensate [6] and susceptibility [5] can be constructed. In section 3.3 we will consider improved estimators for the susceptibilities relevant for the study of superconductivity.

3 Models of Fermions with Spin

There are many ways to construct models of fermions with spin such that the three properties necessary for the meron-cluster method to work, as discussed in section 1.2, are satisfied. The most general approach is to start from the Hamilton operator of interest and proceed with the same steps as discussed in the earlier section. If the Hamilton operator is a sum of only two-fermion interactions, then nothing qualitatively new emerges since it is possible to consider the spin degree of freedom as two "spatial" layers representing up and down spins. All on-site interactions that can occur between the two spin layers can be introduced on a separate time-slice. However, it is now possible to find new reference configurations which are physically meaningful and new models can be constructed using them.

On the other hand, it is natural to allow four-"site" interactions which connect nearest spatial neighbors and the two spin layers. In this case new situations not considered in the previous sections can arise. As an example, consider the transfer matrix element given in figure 6. Although such four-site interactions have not been considered earlier, they can be thought of as two correlated two-site interactions. For example, the shown interaction can arise either due to a "correlated" fermion hop which conserves spin or a "correlated" spin-flip. These two alternatives are shown on the right-hand side in the same figure. If we assume that these new interactions arise from such correlated two-site interactions, then it is possible to use the technology developed for spinless fermions. Here we will take this approach and consider models with four-site interactions.

Instead of trying to find the most general solvable model, we again restrict ourselves to a class of models that can be built with simple correlated two-site interactions. In the next section we will enumerate some of the simplest correlated two-site interactions and in the following section we will build one of the simplest solvable models which has the symmetries of the Hubbard model.

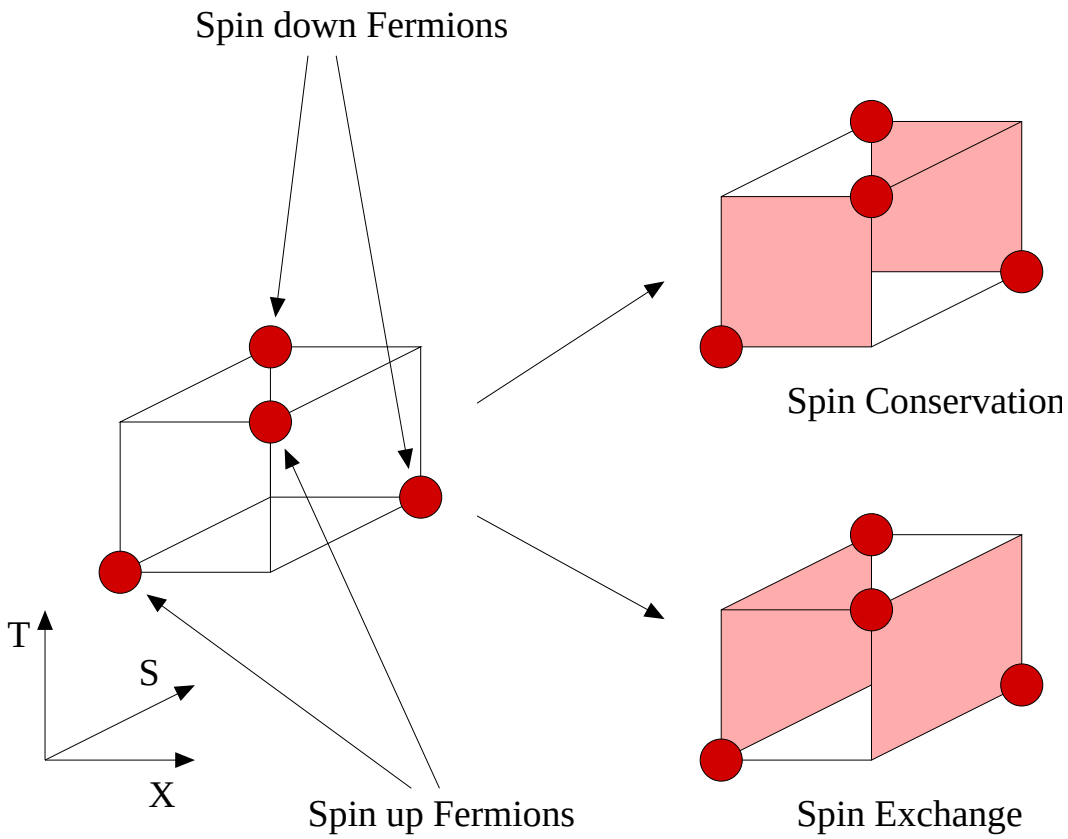

Figure 6: *Configurations with four-site interactions can arise as correlated two-site interactions in different ways. The two possible interactions result in different fermion permutation signs.*

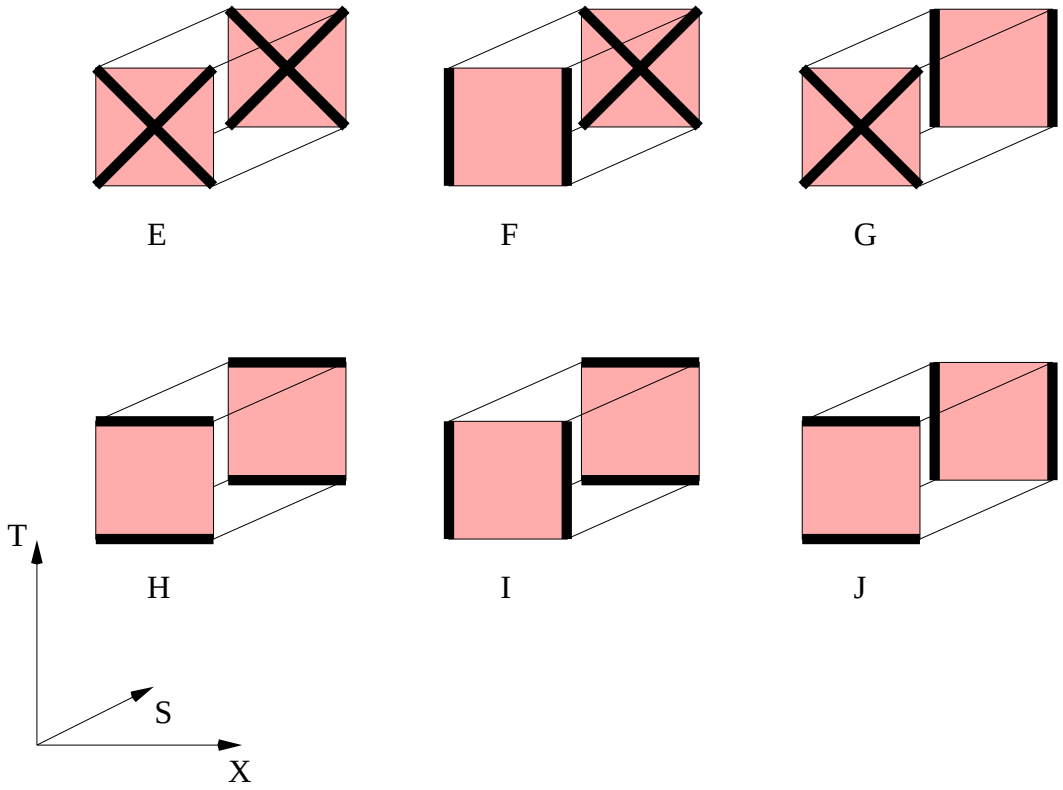

Figure 7: *Spin-conserving bond break-ups that form the building-blocks of models discussed in the text.*

3.1 Building-Blocks of a Cluster Model

Let us first discuss the simplest building-blocks for constructing models of fermions with spin that can be solved using meron-cluster techniques. In the case of spinless fermions, these building-blocks were discussed in section 2.5. There it was shown how these elementary blocks satisfy two of the necessary properties and how one can build models with a reference configuration that ensures that all the criteria of solvability are met. We also discussed how it is possible to find the Hamilton operator for a model that is solvable using the meron-cluster approach. In the case of fermions with spin the various bond break-ups (E, F, G, H, I, J) which conserve spin are shown pictorially in figure 7. In table 2 the transfer matrix elements associated with each of the building-blocks is tabulated. Using the building-blocks it is possible to find models which satisfy all the three required properties of solvability discussed in section 1.2. As an illustration we construct a Hubbard-type model below.

Bond-type	Transfer Matrix
E	$[{c_{x\downarrow}}^\dagger c_{y\downarrow} + {c_{y\downarrow}}^\dagger c_{x\downarrow} - n_{x\downarrow} - n_{y\downarrow} + 1]$
	$\times[{c_{x\uparrow}}^\dagger c_{y\uparrow} + {c_{y\uparrow}}^\dagger c_{x\uparrow} - n_{x\uparrow} - n_{y\uparrow} + 1]$
F	${c_{x\downarrow}}^\dagger c_{y\downarrow} + {c_{y\downarrow}}^\dagger c_{x\downarrow} - n_{x\downarrow} - n_{y\downarrow} + 1$
G	${c_{x\uparrow}}^\dagger c_{y\uparrow} + {c_{y\uparrow}}^\dagger c_{x\uparrow} - n_{x\uparrow} - n_{y\uparrow} + 1$
H	$[{c_{x\downarrow}}^\dagger c_{y\downarrow} + {c_{y\downarrow}}^\dagger c_{x\downarrow} - 2(n_{x\downarrow} - 1/2)(n_{y\downarrow} - 1/2) + 1/2]$
	$\times[{c_{x\uparrow}}^\dagger c_{y\uparrow} + {c_{y\uparrow}}^\dagger c_{x\uparrow} - 2(n_{x\uparrow} - 1/2)(n_{y\uparrow} - 1/2) + 1/2]$
I	${c_{x\downarrow}}^\dagger c_{y\downarrow} + {c_{y\downarrow}}^\dagger c_{x\downarrow} - 2(n_{x\downarrow} - 1/2)(n_{y\downarrow} - 1/2) + 1/2$
J	${c_{x\uparrow}}^\dagger c_{y\uparrow} + {c_{y\uparrow}}^\dagger c_{x\uparrow} - 2(n_{x\uparrow} - 1/2)(n_{y\uparrow} - 1/2) + 1/2$

Table 2: *The operators associated with the building-blocks of spin conserving Hamiltonians shown in figure 7.*

3.2 A Hubbard-Type Model

The Hubbard model is one of the simplest models used to describe superconductivity. In particular, it is believed that the 2-dimensional repulsive Hubbard model may describe the physics of high-T_c cuprate superconductors [17]. The Hamilton operator of the Hubbard model is given by

$$\begin{aligned} H &= \sum_{<xy>,s=\uparrow,\downarrow} \left\{ c^\dagger_{xs} c_{ys} + c^\dagger_{ys} c_{xs} \right\} \\ &\quad + \sum_x \left\{ U \left(n_{x\uparrow} - \frac{1}{2} \right) \left(n_{x\downarrow} - \frac{1}{2} \right) - \mu (n_{x\uparrow} + n_{x\downarrow}) \right\} \end{aligned} \tag{3.1}$$

This model has a global $SU(2)$ spin symmetry whose generators are given by

$$S^+ = \sum_x c^\dagger_{x\uparrow} c_{x\downarrow}, \quad S^- = \sum_x c^\dagger_{x\downarrow} c_{x\uparrow}, \quad S_3 = \frac{1}{2} \sum_x (n_{x\uparrow} - n_{x\downarrow}) \tag{3.2}$$

and a global $SU(2)$ pseudo-spin symmetry at $\mu = 0$ whose generators in two dimensions are given by

$$J^+ = \sum_x (-1)^{x_1+x_2} c^\dagger_{x\uparrow} c^\dagger_{x\downarrow}, \quad J^- = \sum_x (-1)^{x_1+x_2} c_{x\downarrow} c_{x\uparrow}, \quad J_3 = \frac{1}{2} \sum_x (n_{x\uparrow} + n_{x\downarrow} - 1) \tag{3.3}$$

The chemical potential breaks the pseudo-spin symmetry to a $U(1)$ fermion number symmetry. Superconductivity is a result of the spontaneous breaking of this $U(1)$ symmetry. In two dimensions, due to the Mermin-Wagner theorem, it is believed that this symmetry breaking must follow the Kosterlitz-Thouless predictions [18]. For $U < 0$ the theory is expected to show s-wave superconductivity at low temperatures [19, 20]. Then the model can be formulated such that there is no sign problem in traditional quantum Monte Carlo algorithms. However, due to the difficulty of these conventional fermion algorithms the determination of the critical temperature

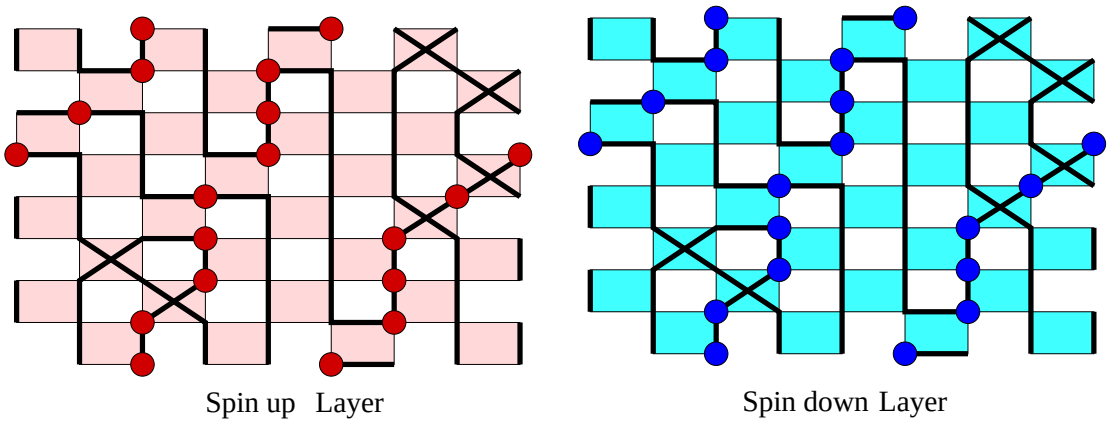

Figure 8: *A typical reference configuration for the Hubbard-type model described in the text.*

is still controversial [21]. The repulsive model with $U > 0$, on the other hand, is more interesting but suffers from a sign problem away from half-filling [1].

Variants of the Hubbard model are equally interesting. For example, the t-J model has also been extensively studied. Here we refer to such models as Hubbard-type models. Let us now construct one such model which is solvable using meron-cluster techniques. The model is based on the four-site transfer matrix elements E and H shown in figure 7. In this model the clusters are identical in the spin-up and the spin-down layers and any configuration of clusters can be flipped into a configuration which is identical in the two layers. Such a configuration always has a positive sign and can hence play the role of a reference configuration. A typical reference configuration is shown in figure 8. Interestingly, unlike in the spinless fermion case, the reference configuration is non-static and not unique. This leads to interesting physical consequences. Another feature of the model is that there are always an even number of meron-clusters: if the cluster in the spin-up layer is a meron then so is the cluster in the spin-down layer.

Using the operators of table 2 the nearest-neighbor Hamilton operator for the model turns out to be

$$\begin{aligned} h_{xy} &= -[{c_{x\downarrow}}^\dagger c_{y\downarrow} + {c_{y\downarrow}}^\dagger c_{x\downarrow} - 2(n_{x\downarrow} - 1/2)(n_{y\downarrow} - 1/2) + 1/2] \\ &\times [{c_{x\uparrow}}^\dagger c_{y\uparrow} + {c_{y\uparrow}}^\dagger c_{x\uparrow} - 2(n_{x\uparrow} - 1/2)(n_{y\uparrow} - 1/2) + 1/2] \\ &- \Delta[{c_{x\downarrow}}^\dagger c_{y\downarrow} + {c_{y\downarrow}}^\dagger c_{x\downarrow} - n_{x\downarrow} - n_{y\downarrow} + 1] \\ &\times [{c_{x\uparrow}}^\dagger c_{y\uparrow} + {c_{y\uparrow}}^\dagger c_{x\uparrow} - n_{x\uparrow} - n_{y\uparrow} + 1]. \end{aligned} \tag{3.4}$$

which leads to the Hamilton operator $H = \sum_{<xy>} h_{xy}$. The operator given in eq.(3.4) can be simplified to [22]

$$h_{xy} = ({c_{xs}}^\dagger c_{ys} + {c_{ys}}^\dagger c_{xs})(n_{xy} - 1)(n_{xy} - 3) + 2(\vec{S}_x \cdot \vec{S}_y + \vec{J}_x \cdot \vec{J}_y)$$

$$
\begin{aligned}
- \quad & 4\left(n_{x\uparrow}-\frac{1}{2}\right)\left(n_{x\downarrow}-\frac{1}{2}\right)\left(n_{y\uparrow}-\frac{1}{2}\right)\left(n_{y\downarrow}-\frac{1}{2}\right) \\
+ \quad & \Delta\left[(c_{xs}{}^{\dagger}c_{ys}+c_{ys}{}^{\dagger}c_{xs})(n_{xy}-2)+2(\vec{S}_x\cdot\vec{S}_y+\vec{J}_x\cdot\vec{J}_y)-4J_x^3J_y^3\right. \\
- \quad & \left.\left(n_{x\uparrow}-\frac{1}{2}\right)\left(n_{x\downarrow}-\frac{1}{2}\right)-\left(n_{y\uparrow}-\frac{1}{2}\right)\left(n_{y\downarrow}-\frac{1}{2}\right)\right], \qquad (3.5)
\end{aligned}
$$

where we have used the definition $n_{xy} = n_{x\uparrow} + n_{x\downarrow} + n_{y\uparrow} + n_{y\downarrow}$. The operators $\vec{S}_x$ and $\vec{J}_x$ are given by the expressions that depend on the site x inside the summation signs in eq.(3.2) and (3.3).

The symmetries of the Hamilton operator given in eq.(3.5) can easily be found. It is interesting to note that the model is invariant under the $SU(2)$ spin symmetry and the $U(1)$ fermion number symmetry. Further for $\Delta = 0$ the $U(1)$ symmetry enhances to the full $SU(2)$ pseudo-spin symmetry. Although unconventional, the physics of this model is closely related to that of the usual attractive Hubbard model. In particular, it was found recently that this model shows s-wave superconductivity even at half-filling [11]. Later we will see that it is possible to add a chemical potential and an on-site attractive interaction to the above Hamiltonian without introducing sign problems. Further, when $\Delta = 0$, it is possible to include an on-site repulsion between the fermions of opposite spin even in the presence of a chemical potential as long as a certain inequality is satisfied. It is interesting to investigate if this "repulsive" model can be a useful candidate for high-T_c superconductivity.

3.3 Improved Estimators

Since the model satisfies all the properties of the meron-cluster approach, its partition function can be expressed purely in terms of clusters,

$$
Z \;=\; \sum_{[b],\mathrm{zero-meron}} 2^{2N_c}\; W[b], \qquad (3.6)
$$

where N_C is the number of clusters on each spin layer. Since the clusters are identical we get an extra factor of two as compared to eq.(2.30). This novel way of re-writing the partition function involves a partial re-summation over cluster-flips and can be extended to other observables as well. We discussed how the deviation of the occupation number from half-filling can be expressed in this new language in section 2.6.

Let us consider observables relevant for s-wave superconductivity. An important observable is the s-wave pair susceptibility

$$
P_L \;=\; \frac{1}{\beta V Z}\int_0^\beta dt\; \mathrm{T}r\left[\,\exp[-(\beta-t)H]\;(p^+ + p^-)\;\exp[-tH]\;(p^+ + p^-)\,\right] \qquad (3.7)
$$

with $p^+ = \sum_x c^\dagger_{x\uparrow} c^\dagger_{x\downarrow}$ the pair creation and $p^- = (p^+)^\dagger$ the pair annihilation operators. An improved estimator for this susceptibility is easy to construct using the results

of [14]. In particular, one can show that non-zero contributions to the two-point correlations arise only if the creation and annihilation operators occur on the same cluster. Further, in the case of the pair susceptibility it is also important that the clusters these operators reside on have been flipped to be identical. The contribution is then proportional to the sum of all possible creation and annihilation points along the cluster. This just gives a factor of the size of the cluster squared. Averaging over the different possible cluster-flips gives for the zero-meron sector

$$\langle P_L \rangle_{\mathrm{cluster-flips,zero-meron}} = \frac{1}{N_t^2 V} \sum_{\mathcal{C}} \frac{1}{2} |\mathcal{C}|^2, \tag{3.8}$$

where $|\mathcal{C}|$ is the size of cluster $\mathcal{C}$. In the two-meron sector we get

$$\langle P_L \rangle_{\mathrm{cluster-flips,two-meron}} = \frac{1}{N_t^2 V} \frac{1}{2} |\mathcal{C}_{\mathrm{meron}}|^2. \tag{3.9}$$

Note that in the two-meron sector there are two identical meron-clusters: one in the spin-up and one in the spin-down layer.

Another observable relevant to superconductivity is the helicity modulus [23, 24] which is defined in terms of the winding number as

$$\Upsilon = \frac{T}{8} \langle W_x^2 + W_y^2 \rangle. \tag{3.10}$$

Here W_x (W_y) is the total number of fermions winding around the spatial boundary in the x- (y-) direction. To measure W_x we need to examine each interaction plaquette crossing the boundary in the x-direction. We count $+1$ for each fermion (up or down spin) that hops across the plaquette in the forward direction, -1 for each that hops in reverse and 0 otherwise. This winding for a plaquette can then be easily expressed in terms of the occupation numbers of the sites touching the plaquette. Consider first just the up spin layer. The winding number on a plaquette that originates from the point x, t and goes in the forward i-direction for one spin layer is

$$W_{x,t,i} = \frac{1}{2} \left(n_{x,t} + n_{x+\hat{i},t+1} - n_{x+\hat{i},t} - n_{x,t+1} \right) \ . \tag{3.11}$$

We can also replace each n above with $n - 1/2$ without changing the results to make the values more symmetric. Now every site counts as $\pm 1/4$ (on a single spin layer) depending on its occupation number and where it is located on the boundary plaquette. Each cluster can then be assigned a spatial winding number which is just the sum of the weights associated with each point on the cluster. Flipping a cluster inverts all the occupation numbers and thus changes the sign of the spatial winding number for that cluster. The total winding number in the x-direction is then a sum over all clusters and both spin layers

$$W_x = \sum_{\mathcal{C}} W_x^{\mathcal{C}\uparrow} + W_x^{\mathcal{C}\downarrow} \ . \tag{3.12}$$

After squaring this we average over all cluster-flips. In the zero-meron sector one obtains

$$\langle W_x^2 \rangle_{\mathrm{cluster-flips,zero-meron}} = \sum_{\mathcal{C}} (W_x^{\mathcal{C}\uparrow})^2 + (W_x^{\mathcal{C}\downarrow})^2 = 2 \sum_{\mathcal{C}} (W_x^{\mathcal{C}\uparrow})^2. \tag{3.13}$$

In the two-meron sector we get

$$\langle W_x^2 \rangle_{\mathrm{cluster-flips,two-meron}} = 2 |W_x^{\mathcal{C}_{\mathrm{meron}}\uparrow}| |W_x^{\mathcal{C}_{\mathrm{meron}}\downarrow}| = 2 (W_x^{\mathcal{C}_{\mathrm{meron}}\uparrow})^2. \tag{3.14}$$

Again, the two-meron sector consists of one meron-cluster in the spin-up layer and one meron-cluster in the spin-down layer both of which are identical.

Using similar procedures it is also possible to calculate other observables like the spin susceptibility which is important to detect magnetic transitions, the d-wave pair susceptibility which is important for high-T_c superconductivity, and various other two-point correlation functions which are of interest. In principle, it is also possible to calculate higher-point correlation functions. However, these will become increasingly noisy and would require more statistics.

3.4 Kosterlitz-Thouless Transitions

As discussed above, the attractive Hubbard model has been studied extensively as a toy model for s-wave superconductivity [20, 21]. It is expected that below a critical temperature transportation of fermion number through the bulk becomes easy, leading to superconductivity (or more appropriately superfluidity since the symmetry is not gauged in the model). In higher dimensions this is related to the spontaneous breaking of the $U(1)$ fermion number symmetry. In two dimensions, since this is forbidden due to the Mermin-Wagner theorem, superconductivity occurs due to the Kosterlitz-Thouless (K-T) phenomena [18].

A variety of striking predictions exist for a K-T transition. For example, at temperatures above the superconducting transition temperature T_c, the pairing susceptibility defined in eq.(3.7) should reach a constant for large enough volumes. As T_c is approached from above this constant should diverge as $\exp(a/\sqrt{T - T_c})$. Below T_c one should be in a phase with long-range correlations such that the finite-volume pair susceptibility diverges as

$$P_L \ \propto \ L^{2-\eta(T)}. \tag{3.15}$$

The critical exponent η equals $1/4$ at T_c and continuously changes to zero as the temperature approaches zero. Unfortunately, none of these have ever been confirmed using conventional algorithms even in the attractive Hubbard model which does not suffer from a sign problem in the conventional formulation.

We propose that the model given in eq.(3.5) is useful for studying the qualitative physics of the attractive Hubbard model since it provides a computational advantage. To illustrate this, recently the finite temperature phase transition in the model

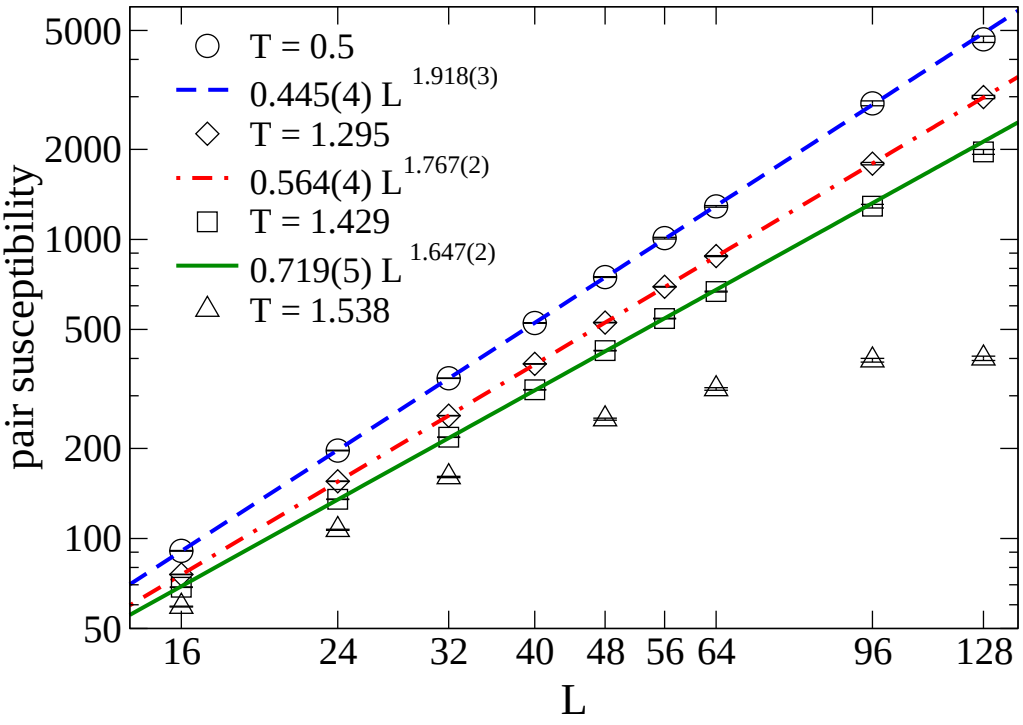

Figure 9: Pair susceptibility as a function of L.

with $\Delta = 1$ was studied [11]. In this case, the Hamilton operator can be re-written as

$$\begin{aligned} H &= \sum_{<xy>} \Big[\sum_{s=\uparrow,\downarrow} (c_{x,s}{}^{\dagger} c_{y,s} + c_{y,s}{}^{\dagger} c_{x,s})(1 - 3n_{xy} + n_{xy}^2) \\ &- 4 \left(n_{x\uparrow} - \frac{1}{2}\right)\left(n_{x\downarrow} - \frac{1}{2}\right)\left(n_{y\uparrow} - \frac{1}{2}\right)\left(n_{y\downarrow} - \frac{1}{2}\right) \\ &+ 4 \left[\vec{S}_x \cdot \vec{S}_y + \vec{J}_x \cdot \vec{J}_y - J_x^3 J_y^3\right] \Big] \\ &- 4 \sum_x \left(n_{x\uparrow} - \frac{1}{2}\right)\left(n_{x\downarrow} - \frac{1}{2}\right). \end{aligned} \tag{3.16}$$

The spin symmetry and the conservation of fermion number is obvious. Further, there is an on-site attraction between electrons of opposite spins like in the attractive Hubbard model. In figure 9 we show results for the pair susceptibility as a function of the spatial size L which demonstrate that the transition in this model indeed belongs to the K-T universality class.

The helicity modulus is also a useful observable to establish the K-T universality class. It can be shown that it satisfies the finite size scaling form

$$\frac{\pi}{T}\Upsilon = 2 + \sqrt{A(T)}\coth\left(\sqrt{A(T)}\log(L/L_0(T))\right), \tag{3.17}$$

with $A(T_c) = 0$ [24]. The helicity modulus has also been measured using the improved estimator discussed earlier and the results further confirm the predictions of Kosterlitz and Thouless. More details can be found in Ref. [11].

3.5 Inclusion of a Chemical Potential

Until now we have only considered models which can be written in terms of clusters that satisfy the three requirements necessary for the meron-cluster techniques to be applicable. However, in certain cases it is possible to relax these stringent requirements and construct models which still have no sign problem. Let us now demonstrate this by extending the Hubbard-type model discussed in section 3.2. We add a single-site term of the form

$$H' = \sum_x \left\{ U \left(n_{x\uparrow} - \frac{1}{2} \right) \left(n_{x\downarrow} - \frac{1}{2} \right) + \mu \left(n_{x\uparrow} + n_{x\downarrow} - 1 \right) \right\}. \tag{3.18}$$

It is easy to see that U induces an on-site repulsion or attraction like in the Hubbard model and μ is just a chemical potential. We have already discussed that in the absence of this single-site term, the partition function of the model is given by

$$Z = \sum_{[b],\text{zero}-\text{meron}} 2^{2N_C} W[b], \tag{3.19}$$

where the origin of 2^{2N_C} can be traced to the four flips of the two identical clusters in the spin-up and the spin-down layer. Further, the reference configuration, obtained when both clusters are flipped identical to each other is guaranteed to be positive. It is straightforward to argue that the above single-site term modifies the factor 2^{2N_C} to

$$\prod_{\mathcal{C}} \left\{ 2 \, \exp\left[-\frac{\epsilon}{2d} \, \frac{U}{4} \, S_{\mathcal{C}} \right] \cosh\left(\frac{\epsilon}{2d} \, \mu \Omega_{\mathcal{C}} \right) \pm 2 \, \exp\left[\frac{\epsilon}{2d} \, \frac{U}{4} \, S_{\mathcal{C}} \right] \right\} \tag{3.20}$$

where $S_{\mathcal{C}}$ is the size of the cluster and $\Omega_{\mathcal{C}}$ is the number of time-slices times the temporal winding number of the cluster. The negative sign should be taken for a meron-cluster.

For the sign problem to remain solved it is important that the factor given in eq.(3.20) remains positive. Clearly, this is the case when $U \leq 0$ for any μ. Interestingly, since the size of the cluster $S_{\mathcal{C}}$ is always greater than or equal to Ω_c, it is possible to show that even when $U > 0$ and $\mu < U/2$ the factor remains positive. This means that we have found a repulsive Hubbard-type model in which it is possible to add a limited chemical potential before the sign problem kicks in. Although it is likely that the interesting physics of high-T_c superconductivity is beyond this region, it appears worthwhile to study this novel model in this region of parameter space where the sign problem remains solved. It is likely that something interesting can be learned there. Finally, in the $U \to \infty$ limit one recovers the Heisenberg anti-ferromagnet. Anti-ferromagnetism is known to be a part of the high-T_c phase diagram.

4 Efficiency of the Meron-Cluster Algorithm

Representing the partition function in terms of the statistical mechanics of clusters interacting locally has the obvious advantage that numerical simulations can become efficient. In this section we compare the efficiency of the meron-cluster algorithm with that of conventional fermion algorithms.

The efficiency of a numerical simulation method can be characterized by the computational cost (the computer time τ) that one must invest in order to reach a given numerical accuracy. Obviously, the cost depends on the d-dimensional spatial volume $V = L^d$, where L is the number of lattice points per direction. In addition, one usually discretizes the Euclidean time-direction of extent $\beta = M\epsilon$ into M time-steps of size ϵ, such that the computational cost increases as one approaches the time continuum limit $\epsilon \to 0$. Besides these two obvious dependences, τ typically also depends on the spatial correlation length ξ via a dynamical exponent z that characterizes the severity of critical slowing down. Further, even if ξ is small, the correlation length ξ_t/ϵ in the time-direction becomes large in units of the temporal lattice spacing ϵ when one approaches the time continuum limit. Hence, there is another dynamical critical exponent z_t that characterizes the corresponding slowing down. Altogether, the total computational cost is typically given by

$$\tau \propto L^x (\beta/\epsilon)^y [c\xi^z + c'(\xi_t/\epsilon)^{z_t}]. \tag{4.1}$$

Standard local algorithms for bosonic systems — for example, the Metropolis algorithm — have $z, z_t \approx 2$. This makes it difficult to simulate systems close to a critical point, i.e. for large ξ, or close to the time continuum limit, i.e. for small ϵ. Local over-relaxation algorithms can be fine-tuned to reach $z, z_t \approx 1$. Efficient non-local cluster algorithms, on the other hand, are far superior because they can reach $z, z_t \approx 0$. Algorithms for bosonic systems typically require a computational effort that increases linearly with the space-time volume, i.e. $x = d$ and $y = 1$. For simulations of fermionic systems this is typically not the case, even when there is no sign problem. Usually, one integrates out the fermions and simulates a bosonic theory with the fermion determinant defining a non-local effective action. The standard fermion algorithm that is most popular in simulations of strongly correlated electron systems [1] computes the determinant of a large matrix of a size proportional to the spatial volume. This requires a computational effort proportional to the spatial volume cubed, i.e. $x = 3d$, even when there is no sign problem, and hence

$$\tau \propto L^{3d} (\beta/\epsilon) [c\xi^2 + c'(\xi_t/\epsilon)^2]. \tag{4.2}$$

A modification of this algorithm proposed in [25] has $x = 2d$. It should be noted that fermion algorithms that have originally been developed for QCD simulations have also been applied to strongly correlated electron systems without a sign problem. The Hybrid Monte Carlo algorithm [26] that was used in [21] has

$$\tau \propto L^{5d/4} (\beta/\epsilon)^{5/4} [c\xi + c'\xi_t/\epsilon], \tag{4.3}$$

and the multi-boson algorithm [27] used in [25] has

$$\tau \propto L^d(\beta/\epsilon)[c\xi + c'\xi_t/\epsilon]. \tag{4.4}$$

Here we have taken the optimistic point of view that one can, at least in principle, reach $z, z_t \approx 1$ by fine-tuning these algorithms. Their computational cost has a much better large volume behavior than the standard algorithm, but they are not necessarily superior on the presently studied moderate size lattices.

When there is a sign problem, the computational cost of the above algorithms increases even exponentially — not just as a power — in the space-time volume. As discussed before,

$$\tau \propto \exp(2\beta V \Delta f), \tag{4.5}$$

such that formally $x = y = \infty$. In practice, this means that systems with a severe sign problem can simply not be simulated. The meron-cluster algorithm allows us to deal with the sign problem extremely efficiently. In particular, the computational cost increases only linearly with the space-time volume, such that $x = d$ and $y = 1$. Still, this does not necessarily mean that we can reach $z \approx 0$ as in cluster simulations of bosonic models. This is due to the re-weighting step in the meron-cluster algorithm. In this step the clusters are locally reconnected such that multi-meron configurations are never generated. For example, a non-meron-cluster may be decomposed into two meron-clusters only if this does not increase the total meron number beyond two. Deciding if a newly generated cluster is a meron naively requires a computational effort proportional to ξ, such that $z \approx 1$ for the meron-cluster algorithm. However, with recent improvements in the implementation we have been able to reduce this effort to only grow with $\log(\xi)$. A nice feature of the meron-cluster algorithm is that — like other cluster algorithms — it can be implemented directly in the Euclidean time continuum [28]. This completely eliminates all time discretization errors and all ϵ-factors in the computational cost. The total computer time that is required to reach a given numerical accuracy with the meron-cluster algorithm is hence given by

$$\tau \propto L^d \beta [c\xi^z + c'(\xi_t/\epsilon)^{z_t}], \tag{4.6}$$

and it is likely that $z, z_t \approx 0$. This is better than standard methods even when there is no sign problem, and exponentially better than any alternative method when there is a severe sign problem.

5 Directions for the Future

In this article we have outlined the essential steps that lead to a novel formulation of fermionic lattice theories. The essential idea behind the new approach is to find a cluster representation of the partition function. We have shown that in

this approach new models can be formulated for which the sign problem can be completely eliminated. Further, although the clusters themselves are non-local they interact locally and carry information about two-point correlations. This makes them especially attractive for numerical simulations. Given the difficulty in the numerical treatment of fermionic theories, this alternative approach turns out to be very useful.

There are many interesting questions that remain unanswered in the case of strongly correlated electron systems. Among these the physics of competing ground states that may exist in high-T_c materials as the doping concentration is increased is one of the most challenging. The model we have constructed appears to have many interesting features that are relevant for this type of questions. This includes anti-ferromagnetism and s-wave superconductivity at the two extremes of the parameter ranges. It would be interesting if this model shows d-wave superconductivity or striped phases in some intermediate range of parameters. Most importantly, the new Hubbard-type Hamilton operator is well suited for numerical work in a large region of parameter space. It would be interesting to study this model in this range. As a first step a mean field analysis may be useful.

The superconductor-insulator transition is another interesting field of research that the present progress may shed some light on [29]. The attractive Hubbard model with disorder has recently been used to study this type of quantum phase transition [30]. We believe that the Hamilton operator of eq.(3.5) with disorder is an alternative model for this purpose. This is possible because the sign problem remains solved in the presence of disorder. Further, since the algorithm for the new model is expected to be much more efficient, it may be possible to go to much smaller temperatures.

It would be interesting to find extensions of the present work to fields like nuclear physics and to nano-science applications like quantum dots. It is easy to construct models with four layers representing spin and isospin which naturally describe the physics of nucleons. It would be useful to construct these explicitly so that we can be sure that the relevant symmetries can be maintained. Extensions of the cluster techniques to models in the continuum is another useful direction. Preliminary work shows that the non-relativistic free fermion model of eq.(2.31) can be extended to the continuum. It would be interesting if this approach can be extended to other interacting non-relativistic free fermions. Such extensions can be useful in studying physics of many electrons enclosed within boundaries as in quantum dots.

Acknowledgments

This work is supported in part by funds provided by the U.S. Department of Energy (D.O.E.) under cooperative research agreements DE-FC02-94ER40818 and DE-FG-

96ER40945, the National Science Foundation under the agreement DMR-0103003 and the European Community's Human Potential Programme under HPRN-CT-2000-00145 Hadrons/Lattice QCD, BBW Nr. 99.0143.

References

[1] S. R. White, D. J. Scalapino, R. L. Sugar, E. Y. Loh, J. E. Gubernatis and R. T. Scalettar, Phys. Rev. B40 (1989) 506.

[2] S. Chandrasekharan and U.-J. Wiese, Phys. Rev. Lett. 83 (1999) 3116.

[3] S. Chandrasekharan, Nucl. Phys. B (Proc. Suppl.) 83-84 (2000) 774.

[4] L. Susskind, Phys. Rev. D16 (1977) 3031.

[5] S. Chandrasekharan, J. Cox, K. Holland and U.-J. Wiese, Nucl. Phys. B576 (2000) 481.

[6] S. Chandrasekharan and J. C. Osborn, Phys. Lett. B496 (2000) 122.

[7] J. Cox and K. Holland, Nucl.Phys. B583 (2000) 331.

[8] U.-J. Wiese, Phys. Lett. B311 (1993) 235.

[9] B. Ammon, H. G. Evertz, N. Kawashima, M. Troyer and B. Frischmuth, Phys. Rev. B58 (1998) 4304.

[10] S. Chandrasekharan and J. Osborn, Springer Proc. Phys. 86, 28 (2000).

[11] S. Chandrasekharan and J. C. Osborn, arXiv:cond-mat/0109424.

[12] W. Bietenholz, A. Pochinsky and U.-J. Wiese, Phys. Rev. Lett. 75 (1995) 4524.

[13] P. Jordan and E. Wigner, Z. Phys. 47 (1928) 631.

[14] R. Brower, S. Chandrasekharan and U.-J. Wiese, Physica A261 (1998) 520.

[15] H. G. Evertz, G. Lana and M. Marcu, Phys. Rev. Lett. 70 (1993) 875.

[16] H. G. Evertz, The loop algorithm, in Numerical Methods for Lattice Quantum Many-Body Problems, ed. D. J. Scalapino, Addison-Wesley Longman, Frontiers in Physics.

[17] See D. J. Scalapino and S. R. White, cond-mat/0007515, for a recent review.

[18] J. M. Kosterlitz and D. J. Thouless, J. Phys. C6 (1973) 1181;
J. M. Kosterlitz, J. Phys. C7 (1974) 1046.

[19] R. T. Scalettar et. al., Phys. Rev. Lett **62** (1989) 1407.

[20] A. Moreo and D. J. Scalapino, Phys. Rev. Lett. 66 (1991) 946.

[21] R. Lacaze, A. Morel, B. Petersson and J. Schroeper , Eur. Phys. J. B2 (1998) 509.

[22] J. C. Osborn, Nucl. Phys. B (Proc. Suppl.) 94 (2001) 865.

[23] E. L. Pollock and D. M. Ceperley, Phys. Rev. B36 (1987) 8343;
H. Weber and P. Minnhagen, Phys. Rev. B37 (1988) 5986.

[24] K. Harada and N. Kawashima, J. Phys. Soc. Jpn. 67 (1998) 2768.

[25] P. Sawicki, Nucl. Phys. B515 (1998) 665.

[26] S. Duane, A. D. Kennedy, B. J. Pendleton and D. Roweth, Phys. Lett. B195 (1987) 216.

[27] M. Lüscher, Nucl. Phys. B418 (1994) 637.

[28] B. B. Beard and U.-J. Wiese, Phys. Rev. Lett. 77 (1996) 5130.

[29] A. Goldman and N. Marković, Physics Today, November 1998.

[30] R. T. Scalettar, N. Trivedi and C. Huscroft, Phys. Rev. B59 (1999) 4364.